NASA
Technical
Paper
2815

April 1988

Rotorcraft Flight-Propulsion Control Integration: An Eclectic Design Concept

James R. Mihaloew,
Mark G. Ballin,
and D. C. G. Ruttledge

NASA

NASA Technical Paper 2815

1988

Rotorcraft Flight-Propulsion Control Integration: An Eclectic Design Concept

James R. Mihaloew
Lewis Research Center
Cleveland, Ohio

Mark G. Ballin
Ames Research Center
Moffett Field, California

D. C. G. Ruttledge
Sikorsky Aircraft Division
United Technologies
Stratford, Connecticut

National Aeronautics and Space Administration

Scientific and Technical Information Division

Summary

The NASA Ames and Lewis Research Centers, in conjunction with the Army Research and Technology Laboratories, have initiated and partially completed a joint research program focused on improving the performance, maneuverability, and operating characteristics of rotorcraft by integrating the flight and propulsion controls. The background of the program, its supporting programs, its goals and objectives, and an approach to accomplish them are discussed in this report. Results of the modern control governor design of the General Electric T700 engine and the Rotorcraft Integrated Flight-Propulsion Control Study, which were key elements of the program, are also presented.

Background

Dynamic-interface problems involving the engine fuel control and the helicopter rotor/airframe have been around for a long time. They include engine torque and fuel control system oscillations, multiengine load sharing, undesirable rotor speed variations during maneuvers, and excessive helicopter vibration. The helicopter rotor and drivetrain system have lightly damped torsional dynamic modes that are within the bandwidth of the engine fuel control system as shown in figure 1. This figure is a bar chart of frequencies at which various dynamic modes commonly occur in rotorcraft. It also shows the frequency ranges involved in rotorcraft design and analysis tasks and that the majority of these tasks require a model that is accurate in a frequency range up to 10 Hz. The trend towards using lower inertia rotor systems in modern helicopters reduces the level of kinetic energy stored in the system and makes the rotor even more susceptible to large variations in its rotational speed during rapid maneuvers. These rotor and speed transients can increase pilot workload and can eventually lead to underutilization of the aircraft's maneuvering capability because of pilot apprehension.

Toward the end of the last decade the U.S. Army Applied Technology Laboratory instituted a contractural program designed to provide a complete report of past and present engine/airframe/drivetrain dynamic-interface problems. The result of this effort was a series of reports from several helicopter airframe manufacturers who documented their specific problems with vehicles developed over the last several years (refs. 1 to 5). The ultimate benefit was to be the accumulation of data that would eventually lead to a solution of these generic dynamic-interaction problems. Although much of the documentation dealt with vibration and oscillatory loading problems related to rotor harmonics excitations, stability and response problems associated with the combining of two or more components or systems were universally stated.

Dynamic-interface problems of this type are among the last to be seen in the design of a subsystem such as an engine since they involve the presence of another subsystem such as a drivetrain and rotor. Designs of both subsystems are often far advanced before the problems are discovered, and in some instances complete subsystems are designed and built before they are integrated on a mechanical basis.

This particular problem is compounded by the fact that both the engine and airframe manufacturers have a detailed familiarization with the characteristics and requirements of their own design, but inadequate knowledge and appreciation for the characteristics and requirements of the other's design or, in particular, the characteristics of the coupled system.

Further compounding of this problem occurs since the analytical approaches used for developing the engine and airframe are unique in assumptions and methodology. As a result, engine manufacturers traditionally tend to use a sophisticated dynamic engine model in conjunction with a rather rudimentary model for the helicopter rotor/airframe dynamics when designing the control system. This is the so-called big-engine, little-airframe approach. On the other hand, helicopter flight dynamicists have traditionally used the opposite approach: that is, the big-airframe, little-engine analysis concept. As a result, the dynamic-interface problems that are not anticipated in the design stage can surface later in the ground or flight test phases of a helicopter development program, requiring costly add-on modifications to "fix" the problems. The prediction and solutions of these problems obviously requires extremely close interaction (complementary interaction, that is) between manufacturers and the several technical disciplines.

In future years, the satisfactory design of fully integrated systems, particularly on a controls basis, will require more coordination among the airframe, engine, and control manufacturers. Success will require an interdisciplinary design approach involving propulsion, dynamics, and handling qualities—all of which should probably be centered within the airframe manufacturers organization. This approach, which basically considers the propulsion system as a highly sophisticated and protected actuator within a flight control system, will, in

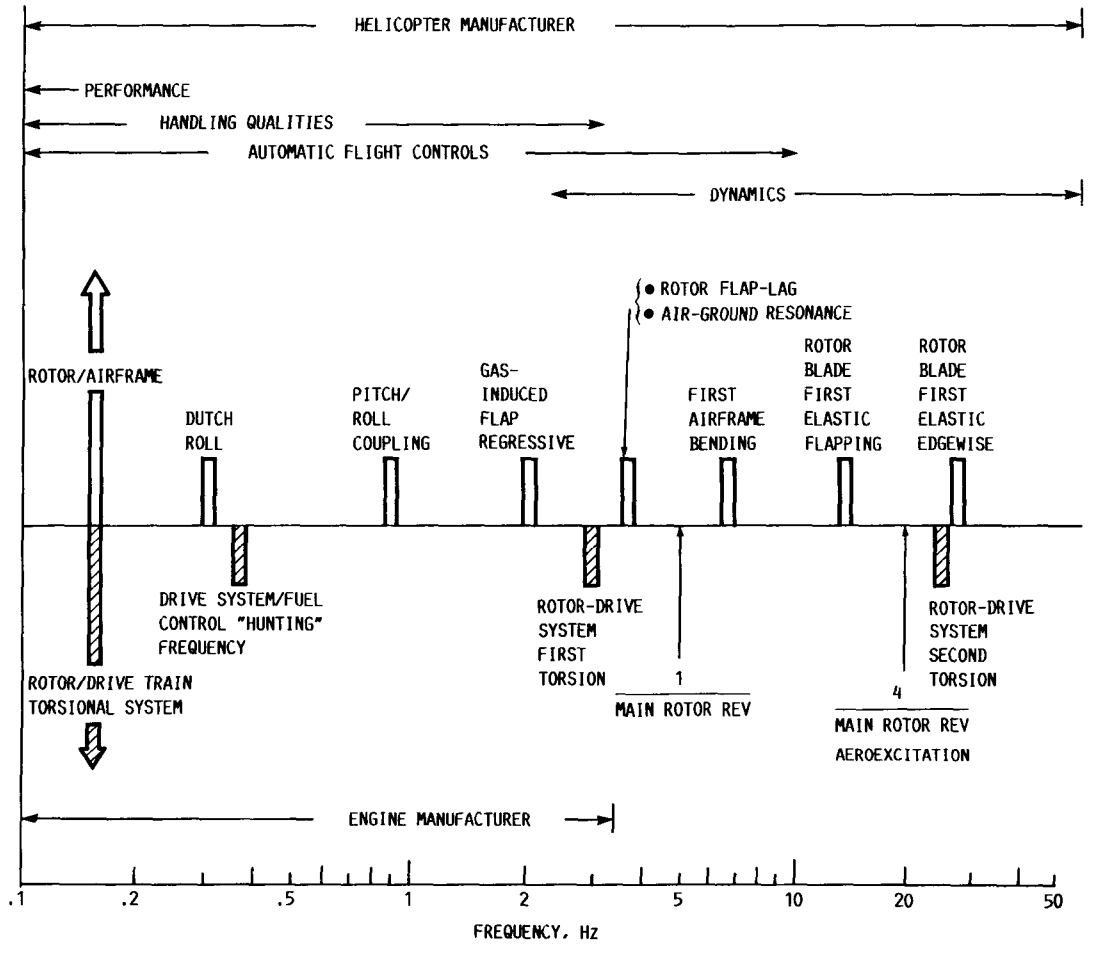

Figure 1.—Modal frequencies of interest in engine fuel control design and modeling.

particular, be necessary for accomplishing integrated flight-propulsion controls.

Flight and Propulsion Control Integration

As mentioned earlier, an increase in the responsiveness of the engine fuel control system using a conventional rotor speed governor can severely compromise the stability margin of the torsional dynamics of the rotor system. Opportunities exist for exploiting the benefits of using integrated, digital flight and propulsion controls, which permit implementation of more sophisticated control logic to improve the dynamic response of the propulsion system and the rotor thrust. For example, the undesirable coupling between the engine fuel control and the airframe/rotor dynamics may be eliminated by employing decoupling control laws and modern multivariable control methodologies. Furthermore, if the power management is appropriately integrated into the flight control system, the engine/fuel control can enhance the performance, maneuverability, and mission capability of the helicopter. The extent to which these benefits can be realized needs to be investigated and demonstrated in flight.

The use of integrated, digital flight and propulsion controls can also expedite the implementation of such active control functions as envelope-limiting and recovery controls in the event of engine failure. An integrated envelope sensing/cueing and system monitoring capability which continuously evaluates the operational environment of the aircraft, the conditions of the airframe and propulsion system, and actively displays status and trend information to the pilot (and/or automatically applies corrective action) will be of significant benefit to single-crew nap-of-the-earth (NOE) operations. The trend of designing today's military helicopters with a higher disc loading and with lighter rotor blades makes autorotation landings more risky than ever before. During entry, descent, and flare phases of autorotation, proper control of the rotor speed is essential, and precise attitude controls are required during the flare and landing phase. Correct piloting techniques are dependent on the altitude and airspeed at the moment when power fails. With integrated, digital flight and propulsion controls, the opportunities now exist to make use of microprocessor technology for onboard, real-time implementation of control and display laws for optimal energy management in the event of engine failure. It warrants, especially in the context of single-crew operations, developing an advanced control and display system

to relieve the pilot of the difficult task of manual control in autorotation. Such controls would permit the pilot to serve primarily as a system monitor only overriding the system when needed.

In the preceding paragraphs, the problems related to the dynamic interface between the engine fuel control and the helicopter rotor/airframe system were discussed, and the needs generated from current missions were described. What opportunities now exist to embark on a program for integrating helicopter flight and propulsion controls? On the flight control and avionics side, the Army has been conducting their Advanced Digital Optical Control System (ADOCS) (ref. 6) and the Advanced Digital Avionics System (ADAS) demonstrator programs using microelectronics and fiber-optics technology. On the propulsion side, full-authority, digital fuel controls have been tested in programs such as the Army Advanced Technology Demonstrator Engine (ATDE). In the area of ground-based simulation and engine test facilities, significant advancement has been made at NASA Ames and NASA Lewis. These research facilities now provide good opportunities to explore the synergistic benefits of integrating digital flight and propulsion controls. The potential benefits include (1) reduced cost and time in development of new rotorcraft through the elimination of engine-airframe dynamic interface problems; (2) enhanced maneuverability, flying qualities, and mission effectiveness; (3) improved fuel efficiency, reliability, and safety; and (4) provision of a data base for rotorcraft procurement specification.

Program Goals and Objectives

The long-term goal of the flight-propulsion control integration program as viewed by NASA is to investigate advanced concepts in digital-active flight-propulsion control, which include (1) improvement of precision flight path control, (2) expansion of the operational flight envelope, and (3) reduction of pilot workload. This goal will be accomplished by applying a systems approach to the design of an integrated flight-propulsion control system to improve performance and handling qualities of the helicopter.

Approach

The program originally consisted of the three phases shown on figure 2. Phase I included modeling and analysis and phase II was concerned with piloted ground-based simulation with integrated flight and propulsion controls. Phase III was a proposed flight hardware and software development program leading to flight evaluations. Phases I and II were part of an ongoing NASA research and technology base program, and phase III was a planned future activity. In executing this program, a coordinated effort was made which involved, in addition to NASA Ames and Lewis Research Centers, the participation of universities, industries, and elements of the Army Aeromechanics and Propulsion Laboratories.

In phase I, effort focused on the development and use of a comprehensive mathematical model for the combined helicopter and engine system for nonreal-time simulation of flight dynamics and parametric studies. A specific helicopter and engine system: that is, an Army-Sikorsky Black Hawk UH-60A with its General Electric T700–GE–701 engines, was used as the baseline. NASA Lewis developed the baseline T700 engine/fuel control system model for integration into the Black Hawk mathematical model. This engine model was correlated and validated by T700 ground tests conducted at NASA Lewis. NASA Ames correlated and validated the total system model with Black Hawk flight test data. The primary research emphasis of this phase of the program was to determine and quantify

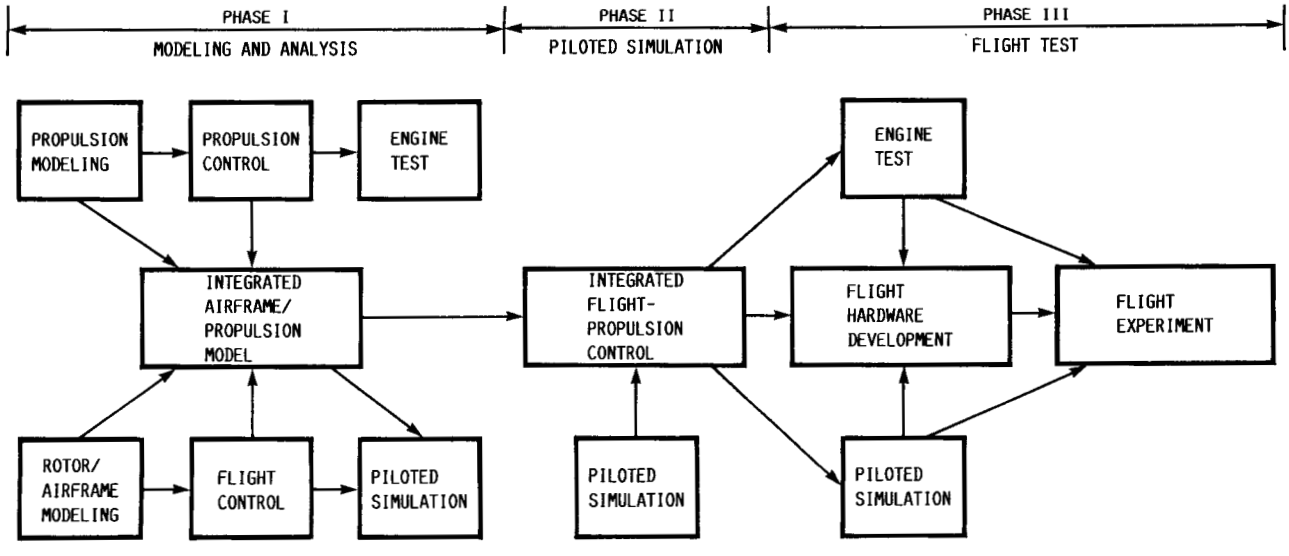

Figure 2.—Rotorcraft flight-propulsion control integration program.

the key parameters that significantly influence the engine/rotor/airframe coupling and overall systems performance. Piloted simulations using both the vehicle and propulsion models developed by the respective flight and propulsion centers were conducted on the Vertical Motion Simulator (VMS) (fig.3) to assess the influences of key system parameters affecting handling qualities for important missions such as NOE flight, helicopter air combat, and search and rescue operations.

Coordinated contract effort and in-house research was pursued in the second phase of the program to develop integrated flight and propulsion control concepts. The contract effort involved a team of engine fuel control specialists and engine and airframe manufacturers. Promising concepts were evaluated on the nonlinear helicopter and engine model over a wide range of flight conditions and then were assessed further using piloted ground-based simulations and engine tests. The merits of each concept were evaluated with respect to handling qualities, pilot workload, maneuver performance, engine performance, and mission capability using representative military and civil mission tasks.

In a future third phase, a research helicopter would be modified to implement the integrated, digital flight-propulsion control system. This vehicle would provide a unique research capability and would be the first helicopter with both digital flight and propulsion controls. Engine ground tests would be conducted at NASA Lewis and piloted ground-based simulations at NASA Ames to verify the control system software and hardware. Flight evaluations of the integrated, digital control system would be conducted using selected tasks from military and civil missions to substantiate benefits, and at the same time, to validate simulation modeling technology. There are no plans at present to initiate or complete phase III activities.

Supporting Programs

Engine Governor Response Study

At NASA Ames, under a collaborative program with the Army Aeromechanics Laboratory, a sequence of piloted simulation experiments were conducted on the VMS to investigate, in a generic sense, the effects of engine response, rotor inertia, rotor speed control, excess power, and vertical sensitivity and damping on helicopter handling qualities in hover and representative low-speed NOE operations (refs. 7

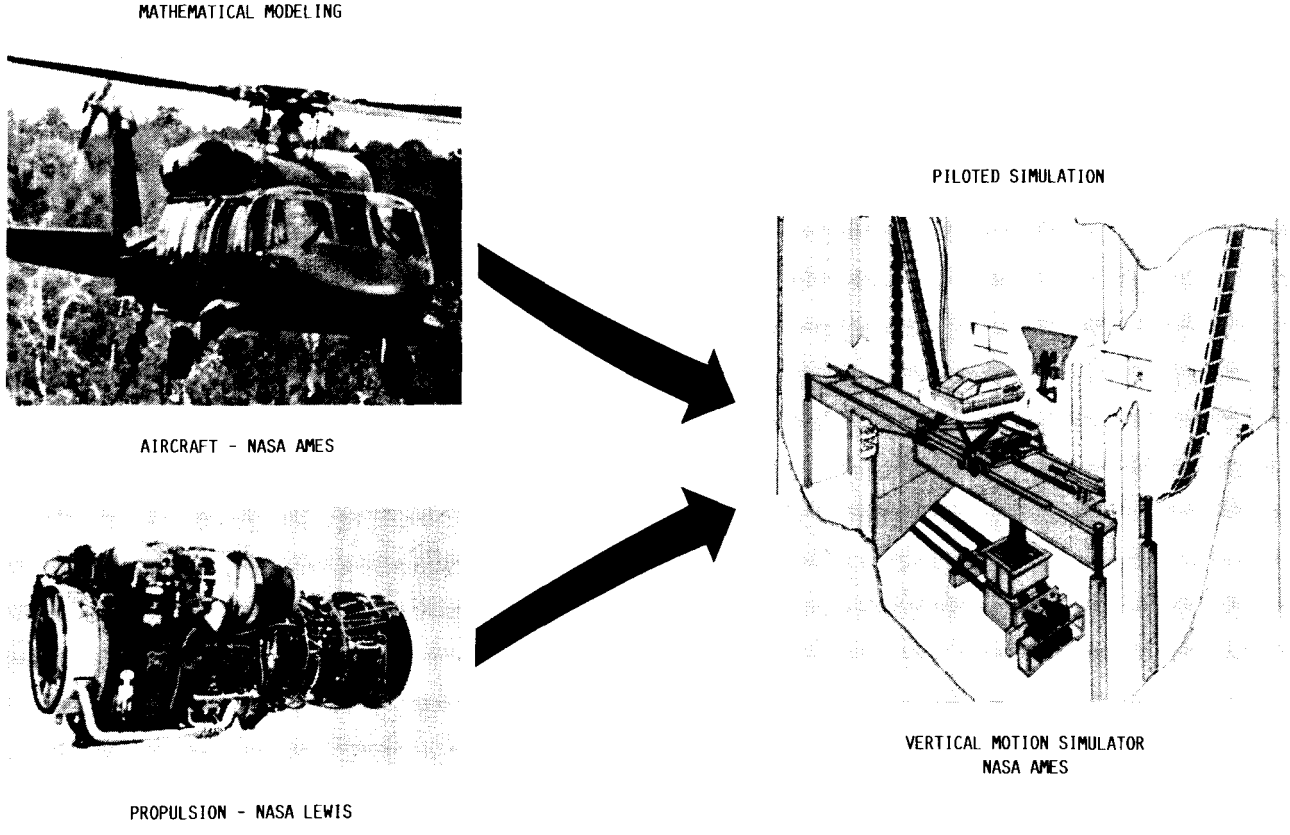

Figure 3.—Rotorcraft flight-propulsion control research—Ames Research Center and Lewis Research Center.

to 9). It was found that variations in the engine governor response time can have a significant effect on helicopter handling qualities as shown in figure 4. Satisfactory (Cooper-Harper pilot rating) handling qualities and rotor speed control were achieved only with a highly responsive governor. An effective engine governor time constant of no more than 0.25 sec was required to achieve a satisfactory level of handling qualities over a wide range of aircraft vertical damping. Increases in the effective engine governor time constant resulted in poor rotor overspeed and underspeed control.

In addition to requiring rapid engine response time, an appropriate level of excess power is required to achieve satisfactory handling qualities for many maneuvers. The excess power requirements for the NOE tasks were investigated with various levels of vehicle vertical damping. In addition to the required engine response time mentioned earlier, an appropriate level of excess power as shown in figure 5 was found to be required to achieve satisfactory handling qualities for the bob-up task evaluated. Results indicated that the required level of excess power is a strong function of the vertical damping and is minimized at a vertical damping of around −0.8 rad/sec.

The thrust response of a helicopter is influenced by several factors including (1) engine governor dynamics, (2) vertical damping resulting from rotor inflow, and (3) the energy stored in the rotor, which is a function of rotor inertia. The experimental results indicated, however, that increase in rotor inertia had only a minor but desirable effect on handling qualities. The effect on handling qualities on requirements for pilot

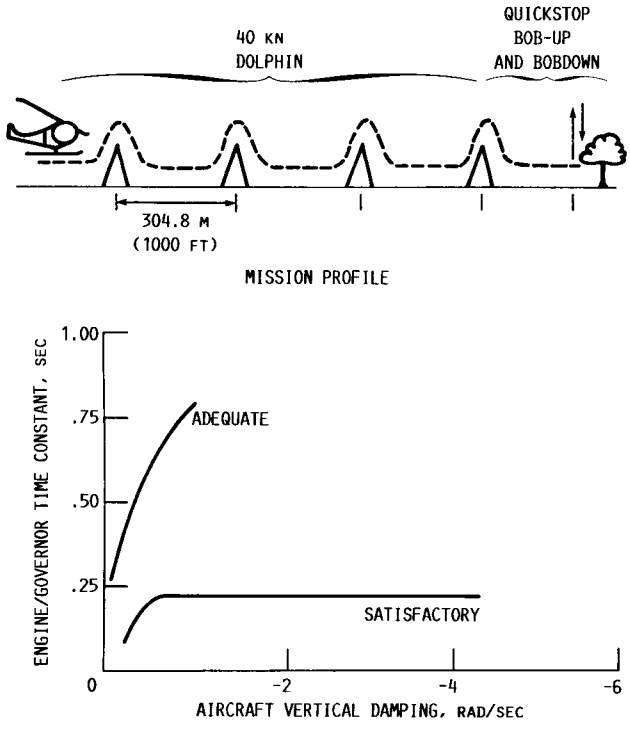

Figure 4.—Effect of engine response on handling qualities.

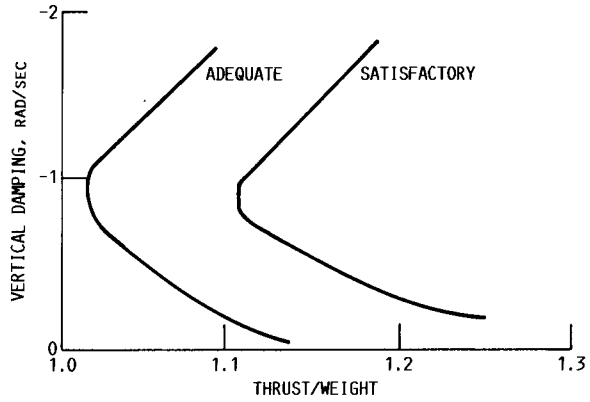

Figure 5.—Effect of excess thrust and vertical damping on handling qualities.

monitoring and control of rotor speed was found to be significant. Thus, techniques to relieve the pilot of the task of monitoring and controlling rotor speed warrant serious consideration.

Small Turbojet Engine Program

NASA Lewis and the Army Research and Technology Laboratory (RTL) Propulsion Laboratory have participated in a cooperative program to conduct digital controls research for small turboshaft engines (ref. 10). The emphasis of the program is on engine test evaluation of advanced modern control logic using a flexible microprocessor-based, digital control system. The digital control system used is designed specifically for research on advanced control logic. Control software is stored in a programmable memory. New control algorithms may be stored in a floppy disk and loaded into the memory to facilitate comparative evaluation of different advanced control modes. Software checkout is accomplished prior to engine test by connecting the digital control to a real-time hybrid simulation of the engine.

The engine used in the facility was a General Electric YT700. The hydromechanical control was modified to allow electrohydraulic fuel metering and variable-guide-vane actuation by the research digital control. The research objective was to demonstrate improved governing of power turbine speed using modern control theory as compared to the baseline control.

Modern Control Governor Design Study

Under the previous program (under contract to NASA Lewis), General Electric recently completed a program using modern control techniques to design a turboshaft speed governor (ref. 11). One of the objectives of this research program was to design a high-performance power turbine speed governor using modern control methods. The power turbine governor was designed using the linear-quadratic-regulator (LQR) method of full state feedback control. A Kalman filter observer was used to estimate helicopter main-rotor-blade velocity.

Figure 6 shows the simulated power turbine speed response to an acceleration caused by a 40- to 70-percent collective-pitch increase in 0.1 sec. The transients were made with the Black Hawk rotor using the nonlinear DISCUS, the manufacturer's reference standard transient model of the T700 engine, without load demand spindle compensation. The results (fig. 6) show that the modern control provides substantially better rotor speed governing than the baseline control. Overall, compared to the baseline T700 power turbine speed governor, the LQR governor reduced droop up to 25 percent for a 490-shp transient in 0.1 sec simulating a wind gust, and up to 85 percent for a 700-shp transient in 0.5 sec simulating a large collective-pitch-angle transient. Unfortunately, the control design was never evaluated experimentally since the program was terminated at NASA Lewis. This technique is discussed more fully later in this report.

Adaptive Fuel Control Program

The Adaptive Fuel Control program, sponsored by the Army Advanced Technology Lab (ATL) Research and Technology Laboratories, was an outgrowth of the full-authority, digital electronic control used on the ATDE (refs. 12 to 14). The objective of phase I, the feasibility investigation, was to determine the feasibility of designing an electronic control capable of adapting its control characteristics while in operation to optimize engine performance. The first step was to identify the prospective adaptive concepts to be investigated and then analyze them using a flight dynamics simulation. The concepts which proved feasible were incorporated into a preliminary design. Phase II of the program was to use the results of phase I to fabricate an electronic control and to conduct bench and engine tests. Phase III is a current activity of the program which brings the adaptive controller into a flight test program. The objective of phase III is to verify the performance of the adaptive control during flight for expected improvements in maneuverability, engine control, torsional stability, and pilot workload. In addition, the modern control concept discussed previously will also be evaluated.

The Adaptive Fuel Control program has identified significant benefits in agility and pilot workload through the use of several digital fuel control elements for improved rotor speed governing. References 12 to 14 present the results of the program to date. For combined aircraft and propulsion control

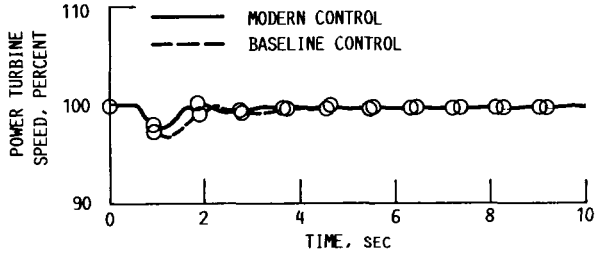

Figure 6.—Uncompensated engine acceleration transient caused by a 40- to 70-percent collective-pitch burst.

simulations, improvements in handling qualities and vehicle performance were noted. For example, tests showed significantly reduced rotor speed droop following power recovery from autorotation. The Adaptive Fuel Control study also identified a significant benefit from variable rotor speed during cruise. Rotor speed optimization was found to reduce fuel consumption by 5 to 10 percent for some cruise conditions. Although the focus of the Adaptive Fuel Control program is on improved propulsion controls, the program also provides a strong basis for further work on integrated flight-propulsion control.

Rotorcraft Integrated Flight-Propulsion Control Study

With the advent of the use of fast microprocessors for the control of various subsystems on aircraft, a need arose to investigate the synergism associated with integration of the various independent control elements and concepts. In addition, as a result of efforts such as the Army ADOCS program, digital flight controls will be employed in the next generation of advanced rotorcraft. Similarly, as a result of efforts such as the Army ATDE and Adaptive Fuel Control programs, digital propulsion control is now emerging in operational rotorcraft systems. The next logical step in the progression is to consider vehicles that will have both digital flight controls and digital propulsion controls and to identify the benefits in mission performance for a fully integrated, digital flight-propulsion control system. As a part of satisfying that need, NASA Lewis has contracted with Sikorsky to investigate the benefits of integrating the flight and propulsion control systems in helicopters. The Black Hawk helicopter with T700 engines is used as a typical modern rotorcraft for this effort because state-of-the-art vehicle and propulsion simulations were available for domestic dissemination.

Sikorsky Aircraft conducted a study whose primary objective was the identification of the benefits associated with an integrated flight-propulsion control system for rotorcraft. This was accomplished by designing a system following appropriate concept screening, incorporating and evaluating the integrated control in a NASA-supplied Black Hawk and T700 simulation, and recommending experiments to be conducted by NASA using the VMS at NASA Ames with their modified Black Hawk simulation. The work was performed at Sikorsky and was supported by General Electric and the Chandler Evans Division of Colt Industries. The balance of this report is a summary of that work. A complete report is given in reference 15.

Study Summary

An eclectic approach, as opposed to a global approach, was taken in a study of the integration of digital flight and propulsion controls for helicopters. The basis of the evaluation was a current simulation of the UH-60A Black Hawk

helicopter with a model of the General Electric T700–GE–701 engine developed by NASA. Initial design work of the fuel control for the integrated control was performed using the COPTR simulation of Chandler Evans. COPTR is a simulation of a generalized, twin-engine-powered helicopter employing a highly detailed and flexible fuel control, fuel-transfer system, and engine model coupled to an adequately representative airframe model. Subsequent design iterations were made using Sikorsky's Master Generic Helicopter (MGH) facility.

A list of segments of flight maneuvers to be used to evaluate the effectiveness of the resulting integrated control system was composed based on past experience and an extensive survey of the recently acquired U.S. Army Air-to-Air Combat Test (AACT) data.

A number of possible features of an integrated system were examined. Those chosen were combined into a design that replaced the T700 fuel control and part of the Black Hawk control system. This design consisted of portions of an existing pragmative adaptive fuel control design by Chandler Evans and an LQR-based power turbine governor design by General Electric. These design features were melded with changes in the baseline Sikorsky flight control system.

A cursory assessment of the design is presented here. Overall, the integrated system exhibited superior total system performance in many areas of the flight envelope primarily because of the LQR power turbine governor. A more extensive investigation is needed on the NASA Ames VMS to confirm this result.

Aircraft Modeling

Description of the Black Hawk helicopter.—The UH–60A Black Hawk, as shown in figure 7, is a utility transport helicopter developed by Sikorsky for the Army. This medium-sized helicopter is designed to carry 11 combat-equipped troops and a crew of three. The basic structural design gross weight is 16 825 lb with a maximum alternate gross weight of 20 500 lb. Missions include troop assault, aeromedical evacuation, aerial recovery, and extended range missions. The Black Hawk has a maximum level flight speed in excess of 160 kn and a diving speed in excess of 170 kn.

The Black Hawk has a single main rotor and a canted tail rotor. The main rotor consists of four fully articulated titanium-fiberglass blades that are retained by a flexible elastomeric bearing in a forged titanium single-piece hub and are restrained by a conventional hydraulic lag damper. The 11-ft-diameter four-bladed tail rotor is a bearingless cross-beam arrangement with the shaft tilted 20° upward. Both rotors have the same aerofoil section. The aircraft is powered by two General Electric T700–GE–700 engines mounted on top of the cabin. Together these engines provide approximately 2800 hp at normal continuous rating. These engines have Hamilton Standard hydraulic and General Electric electronic fuel controls. The drivetrain consists of main, intermediate, and tail gear boxes with interconnecting shafts.

The baseline flight control system on the Black Hawk is a redundant hydroelectrical-mechanical system. It includes three two-stage main-rotor servos, a stability augmentation system, a flight path stability system, and a triple redundant hydraulic supply. The horizontal tail rotates from a positive angle of about 40° in hover to −8° with increasing forward speed.

Simulation model.—The mathematical model of the Black Hawk is a generalized and modularized analytical representation of a total helicopter system developed under Sikorsky's MGH system (ref. 16). It normally operates in the time domain and allows the simulation of any steady or maneuvering condition that can be experienced by a pilot. The solution in terms of aircraft motion is obtained iteratively by summing the component forces and moments acting at the aircraft's center of gravity and subsequently obtaining the accelerations of the body axes. Resulting velocities and displacements then condition the environment for the components on the next pass through the program.

The basic model is a total force, nonlinear, large-angle representation in six rigid degrees of freedom. In addition, rigid rotor blade flapping, lagging, and hub rotational degrees

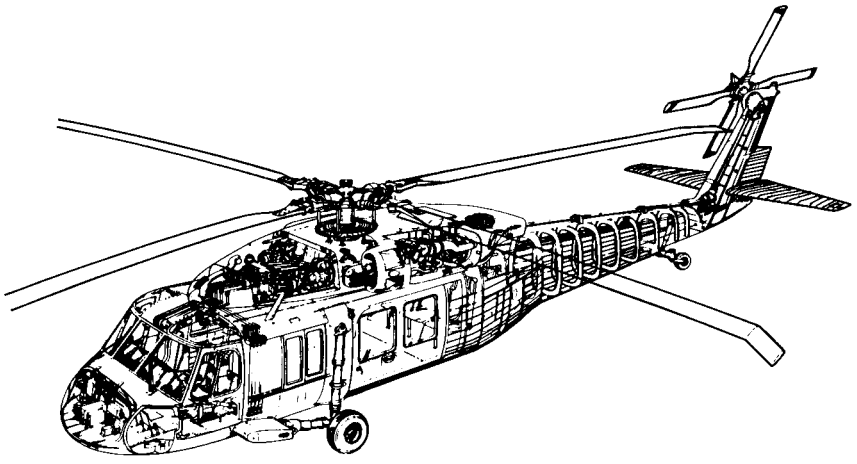

Figure 7.—Sikorsky UH–60A Black Hawk helicopter.

of freedom are represented. The latter degree of freedom is coupled to the engine and fuel control. Motion in the lag degree of freedom is resisted by a nonlinear lag damper model.

The total rotor forces and moments are developed from a combination of the aerodynamic, mass, and inertia loads acting on each simulated blade. The rotor aerodynamics are developed using a blade element approach. The angle of attack and the dynamic pressure on individual blade segments are determined from the three orthogonal velocity components. These arise as a result of airframe motion, rotor speed, blade motion, and downwash resulting from the generation of thrust. In the latter case, which represents the air-mass degree of freedom, a uniform downwash is derived from momentum considerations, passed through a first-order lag, and then distributed harmonically first as a function of rotor wake skew and the aerodynamic hub moment. Finally, blade geometric pitch is summed with the inflow angle of attack at the blade segment. The full angle of attack range for blade aerodynamics is represented as a function of Mach number.

Blade inertia, mass, and weight effects are fully accounted for and their resulting loads, dependent on blade and aircraft motion, are added to the aerodynamic loads for each blade. This summation gives the shear loads on the blade-root hinge pins. Total rotor forces are obtained by summing all the blade hinge-pin shears with regard to azimuth. Rotor moments result from the offset of the hinge shears from the center of the shaft. Blade flapping and lagging motion is determined from aerodynamic and inertia moments about the hinge pins. During one pass through the program all segments and all simulated blades are computed. If because of execution time considerations the simulated number of blades are not made equal to the actual number, then they are redistributed in azimuth accordingly.

The fuselage is defined by six component aerodynamic characteristics that are loaded from wind tunnel data extended analytically to large angles. The angle of attack at the fuselage is developed from the free stream plus the interference effects from the rotor. These interference effects are based on rotor loading and rotor-wake skew angle. Local velocity effects are not accounted for.

The aerodynamics of the empennage are treated separately from the forward airframe. This separate formulation allows definition of nonlinear tail characteristics that would otherwise be lost in the simplifications of multivariate total aircraft maps. With this approach, changes to the empennage can be made without reloading basic airframe maps. The angles of attack at the empennage are developed from the free-stream velocity plus the rotor wash and airframe wash. Dynamic pressure effects from the airframe are accounted for by factoring the free-stream velocity component. By necessity the wash and dynamic effects are averaged over the stabilizing surfaces. The tail rotor is represented by the Wheatley-Bailey theory solution. The airflow encountered by the tail rotor is developed in the same manner as the empennage. An empirical blockage factor due to the proximity of the vertical tail is applied to the thrust output.

The baseline Black Hawk flight-control system presented in this model covers the primary mechanical flight control system and the automatic flight control system (AFCS). The latter incorporates the stability augmentation system (SAS), the pitch bias actuator (PBA), the flight path stabilization (FPS), and the stabilator mechanization. These automatic control functions collectively enhance the stability and control characteristics of the vehicle. The analytical definition of the control system incorporates the sensors, shaping networks, logic switching, authority limits, and actuators. Some of these components have wide bandwidths that are beyond the frequencies normally associated with piloted simulation. They have been included for completeness and accuracy in analytical evaluations. The model provided represents the control system in a complete manner except for the FPS. In this case, only the attitude hold and turn features have been defined.

The aircraft model also includes a landing interface module which allows for ground contact, a simplified ground effects model, and a gust-penetration routine that provides for a gust front passing across the rotor disc from any direction.

Model Correlation.—The present MGH representation of the Black Hawk has been correlated with flight test data at a frequency range of 0 to 4 Hz. At 0 Hz, the small number of blade segments and lack of performance details prevents the use of MGH for predicting performance. However, trim attitudes and control positions are adequately forecast. At frequencies above about 5 Hz, the present MGH modules do not model the rotor dynamics well enough to predict performance. The actual computation frequency of MGH for stability considerations is 50 to 100 Hz. Thus detailed AFCS design and blade-stability investigations are outside the useful range of MGH while primary control systems, simple SAS, and first engine-rotor torsional oscillation studies are well within it.

Propulsion System Modeling

The accurate representation of propulsion system performance and dynamic response to changing load conditions is becoming an important component in experimental handling qualities investigations. A high level of sophistication in modeling the powerplant, drivetrain, and all power requirements of the vehicle is necessary to achieve an accurate representation of vehicle performance and dynamic response, especially for such demanding mission tasks as NOE flight. It is also important in simulating off-design vehicle configurations and in exploring expanded mission requirements for a particular vehicle. Piloted simulation has the advantage of efficiently determining requirements made on the propulsion system as well as the response of the pilot to the interaction of the propulsion system with the vehicle.

High-fidelity propulsion system modeling is particularly necessary in the investigation of integrated flight and propulsion controls for rotorcraft. Because advanced propulsion control strategies may involve monitoring or estimation of internal engine states, an accurate internal representation of the engine is required. In addition, much dynamic interaction between the rotor, drivetrain, and propulsion system takes place at the once-per-revolution frequency of the rotor (ref. 17). The present generation of real-time blade-element rotor-helicopter simulations such as GENHEL, a general helicopter predecessor of MGH, is able to accurately model individual blade dynamics at such a bandwidth. A real-time model which correctly represents propulsion system dynamic response at a high bandwidth is therefore necessary. Because rotorcraft-propulsion system load demand varies typically from zero power to full power, the model must be valid over the full power range of the actual engine. It must be valid over a complete range of ambient operating conditions. Engine parameters of primary importance to real-time handling qualities investigations include output torque and dynamics of the gas turbines, which are necessary for pilot sound cueing as well as for modeling of power output. Also important are parameters used by the fuel control system, such as compressor discharge static pressure and internal engine temperatures. Of somewhat less importance are the internal mass flows, which may be used to determine proximity to limits such as compressor stall.

Available real-time models are based on simple power-versus-fuel-flow relationships, or, in more sophisticated models, engine dynamics are based on experimentally determined partial derivatives of changes of output torque to changes in turbine speed and fuel flow. Such models are unsatisfactory because needed internal engine states may not be modeled. In addition, dynamic characteristics of existing models have shown poor results in validation with experimental data (ref. 18). Partial derivative models tend to be valid only for a limited range of operating conditions. Because these models are not based on the physical phenomena they represent, their validity is always in question when they are used under suboptimal conditions.

An acceptable level of fidelity can be achieved by using an engine model made up of individual engine components, each of which is modeled based on physical laws relating the dynamics of mass flow and the transfer of energy. Such individual-component simulations are used by engine manufacturers to study the transient behavior of engines, but they are usually far too complex for use in real-time digital simulation. A component engine model that is simplified for real-time use is the most promising alternative to partial-derivative engine representations. It was therefore chosen to be appropriate for the study of flight and propulsion controls integration.

In addition to a sophisticated engine model, accurate physical models of the fuel control system, mechanical actuators and linkages, and the engine sensors are necessary for a correct representation of closed-loop propulsion system dynamics, engine protection control, and the effects of modification of the propulsion system control. Similarly, the vehicle drivetrain and accessory loads must be modeled so that an acceptable representation of the power requirements of the vehicle is obtained.

Engine and drivetrain description.—The engine modeled (fig. 8) is a General Electric T700–GE–701, a small turboshaft engine of the 1500-hp class used in the UH–60A Black Hawk and the AH–64 Apache helicopters. It consists of a five-stage axial and a single-stage centrifugal flow compressor, a low-fuel-pressure through-flow annular combustion chamber, a two-stage axial gas generator turbine, and a two-stage independent power turbine. (Data obtained from Model Specification for T700–GE–701 Turboshaft Engine. Part I. DARCOM–CP–2222–02701, Feb. 1983.) The first two stages of the compressor use variable-geometry inlet guide vanes and stator vanes, and air is bled from the compressor exit to cool the gas generator turbine. The power turbine has a coaxial driveshaft that extends forward through the front of the engine where it is connected to the output shaft assembly.

The T700 fuel control system provides power modulation for speed control, overtemperature protection, and load sharing between engines for multiple-engine installations. It consists of a hydromechanical control unit (HMU) for fuel metering (as a function of schedules of gas generator speed and power demand) and an electrical control unit (ECU) that performs isochronous power turbine speed governing and over-temperature protection. (Data obtained from Prescott, W.E.; and Mabee R.L.: T700–GE–701 Training Guide. General Electric Aircraft Engine Business Group, Lynn, MA, 1984.) The HMU consists of a high-pressure vane pump and mechanical cams which impose acceleration, deceleration, topping, and idle schedules as functions of inlet temperature and gas generator speed. A feed-forward compensation of load demand is achieved by adjusting the set point as a function of collective control. The compressor variable geometry is also controlled as a function of inlet temperature and gas generator

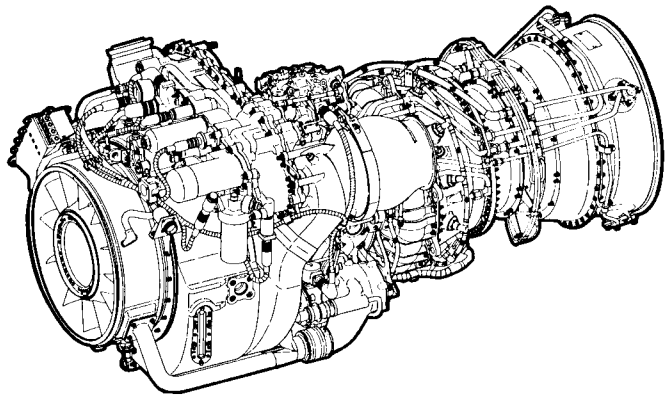

Figure 8.—General Electric T700–GE–701 turboshaft engine.

speed. The ECU provides output shaft speed control by driving a torque motor in the HMU based on a power turbine speed error signal. The torque motor adjusts the HMU fuel demand downward so that an electrical system failure results in maximum power. Power turbine inlet temperature is also monitored and fuel flow is reduced when it exceeds limits. Power may also be increased if torque is determined to be lower than that of another engine operating in parallel.

The UH–60A drivetrain consists of a transmission that reduces engine shaft speed and transfers power to the main-rotor, intermediate, and tail gearboxes that, in turn, transfer power to the tail rotor and freewheeling clutches. The transmission receives torque from each engine through input bevel gears and through an overrunning clutch that allows the gearbox speed to exceed that of the engine output shaft as may occur during autorotation or an engine-out situation. A set of planetary gears then transmits torque to the main-rotor shaft and to the intermediate gearbox. Accessory loads that also receive power from the transmission include a transmission oil cooler fan, hydraulic pumps, and generators. They are driven from the main bevel via additional bevel and spur gears.

Engine model.—As a part of ongoing research in turboshaft engine technology, an individual-component type mathematical model was developed by NASA Lewis for real-time hybrid computer simulation (ref. 19). It is a greatly simplified version of the component-type cycle-deck analysis program developed by the manufacturer, and, although it is inappropriate for engine development purposes, it is at a level of sophistication necessary to model the operating condition of the engine as well as engine transient behavior. This program was chosen as the basis for developing a real-time digital simulation adequate to use with real-time blade-element rotorcraft simulations.

A diagram of the major components separated by mixing volumes is shown in figure 9. The four major components are separated by fluid mixing volumes, each of which is associated with flow passages within the engine where thermodynamic states are quantifiable. States of the gas in each control volume are expressed in terms of pressure, temperature, and mass flow. They are determined as functions of energy transfer across each component. Equations describe each component in terms of the component state, thermodynamic states upstream and downstream of the component, energy applied to or from the component, and efficiencies of energy transfer. Dynamics of the rotating components are modeled by relating changes of angular rotation of a given component to its moment of inertia and the applied torque. A load from an external source is required to determine power turbine and output shaft speed. Losses associated with fluid dynamic or mechanical processes are represented by single or multivariable functions based on previously derived or empirical data. Inputs to the simulation are ambient temperature and pressure at the inlet, pressure at the exhaust, and fuel flow.

Modeling simplifications made in the development of the NASA Lewis hybrid simulation model were based on a general simulation technique developed at NASA Lewis (ref. 20) as well as on experience with small turboshaft engines. Power turbine efficiency as a function of its speed was neglected because, for the designed use of the model, the power turbine deviates only a few percent from its design speed. No modeling of compressor surge, heat-sink losses, or exhaust pressure losses was attempted. Linear relationships were used to describe secondary effects such as bleed flows. Dynamics of the variable geometry guide vanes were assumed to be instantaneous. A digital program was then produced using the Continuous System Modeling Program (CSMP) which accurately reproduced steady-state operation of an experimental test article operated at NASA Lewis. Finally, a real-time fixed-point hybrid version of this program was written to interface with control system hardware. Because of the lack

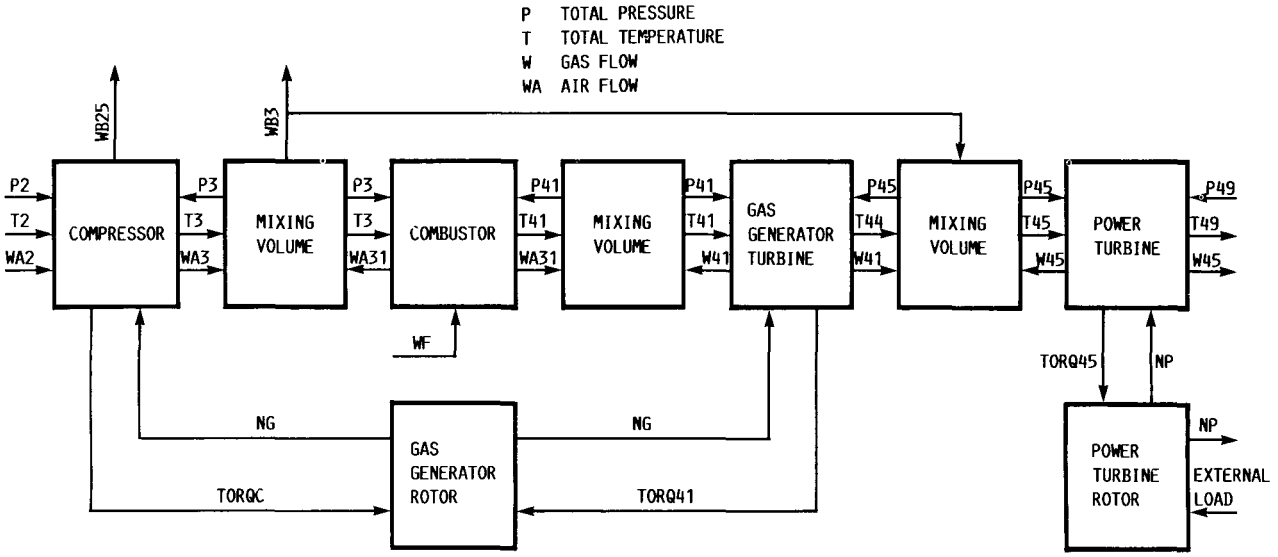

Figure 9.—Block diagram of small turboshaft engine model.

of transient data, no validation of engine dynamic characteristics was performed in this phase of the model development (ref. 19).

In the development of a real-time digital model, the CSMP model was used as a basis for developing a program in FORTRAN using real-time digital programming methods. Transfer functions were modeled using a zero-order-hold state-space formulation when possible and a Tustin formulation if numerical stability was a factor. During the validation, it was discovered that the original model contained too much simplification to correctly model engine dynamics. Consultation with the engine manufacturer resulted in the addition of models for losses caused by heat dissipation within the gas generator and exhaust flow downstream of the power turbine. A model of power turbine efficiency as a function of its speed was also found to be necessary to model the low-power closed-loop dynamic response properly. The HMU required the addition of metering valve and collective anticipation lags, fuel transport delay, combustor lag, and models of sensor hysteresis. The ECU also required a more sophisticated model of torque motor dynamics.

Drivetrain model.—The drivetrain model is at a simplified level of sophistication appropriate for use with the real-time blade-element rotor program. The gearbox is represented as a ring gear that receives torque from the engines, performs gear reduction, and distributes power to the main-rotor, tail-rotor, and accessory loads. In real-time use, output from one engine is used to represent both engines by doubling the value of shaft torque. Change of gearbox speed is determined as a function of the net applied torque and inertias of all rotating loads, transferred to the rotating speed of the gearbox. Estimates are made of drivetrain damping caused by transmission oil lubrication and friction losses. Each freewheeling clutch is modeled to disengage if the gearbox-required torque is less than zero and to reengage if the engine shaft speed exceeds that of the gearbox. Elastically deformable driveshafts are not represented in the real-time version.

Real-time implementation.—Each of the control volumes within the engine is associated with a temperature, pressure, and change of mass of the air and fuel. During steady-state operation of the engine, a state of equilibrium exists between the control volumes for each of these parameters.

A change in the state of any control volume creates pressure and mass flow changes in the other control volumes until a new equilibrium is achieved. The dynamics associated with this change are very rapid; that is, they have a negligible effect on the lower frequency engine and vehicle dynamics. Discrete modeling of such high-frequency dynamics necessitates stepping forward in time with extremely small increments, resulting in a high computation overhead unacceptable for real-time simulation.

A quasi-static approximation of the volume dynamics of the engine was therefore made. High-speed dynamics were eliminated by approximating equilibrium states at all times for the pressures and mass flow within the mixing volumes. By developing linear small-perturbation versions of the component model, we verified that the approximation had little influence on lower frequency dynamics. A central-difference extraction method was used to estimate stability derivatives for a six-state model and for a reduced-order three-state linear representation for several operating points. An eigenanalysis of these models suggested that the lower frequency turbine speed and heat-sink states are affected to a negligible degree by elimination of the three volume-dynamic states.

The omission of dynamic states leads to sets of coupled algebraic equations that cause discrete modeling errors. Because look-up tables are required for the nonlinear functions, the equations may not be solved simultaneously: iteration methods must be used. For real-time simulation, excessive amounts of iteration (ref. 21) must be avoided to limit computational demands. Also, because the time step is generally not variable for real-time simulation, it must be chosen based on the maximum number of iterations needed, resulting in poor computational efficiency. A further complication is caused by the large time increments used by real-time simulations. They may cause large changes of the engine states between intervals, thus necessitating an optimal convergence of the iteration for accuracy and numerical stability.

Several existing real-time and nonreal-time computer models of turbojet engines use a quasi-static volume dynamics approximation (refs. 21 to 23). Methods differ in the application of this numerical scheme, which allows an iterative convergence to equilibrium with a minimum use of computation time. An opened iteration scheme is normally used, sometimes in conjunction with a set of predetermined partial derivatives of engine states. However, an opened iteration does not allow control of convergence or of the amount of error produced.

A fixed-point iteration method was found to meet the requirements of computational efficiency and small error. A successive overrelaxation technique was used to control the speed of convergence. Only 10 iterations of two small parts of the program, corresponding to 110 arithmetic operations, were found to be necessary for convergence to within 0.1 percent under the most extreme transient power conditions.

Validation.—Steady-state engine performance was verified to be within normal limits of operation by comparison with the experimental engine operated by NASA Lewis and with DISCUS, the performance standard component model program developed by the engine manufacturer. Loading conditions were duplicated by using a model of the NASA Lewis test engine dynamometer described in reference 10. The load is variable based on a simulated collective-pitch-control input. This input is used to trim the engine at the design shaft speed for a specified fuel flow. Excellent agreement was obtained with the manufacturer's model. Gas generator speed was found to have a maximum error of one percent while output torque error was less than 4 percent. Hot-section temperatures also correlated well with a maximum error in gas generator inlet temperature of less than 1 percent with a corresponding error

in power turbine inlet temperature of slightly over 1 percent. Comparison of the real-time model with the NASA experimental engine test resulted in in fair agreement. The experimental engine is a prototype model that does not reproduce specification performance. Real-time model turbine speeds were within 3 percent of the test engine speeds. However, temperatures at the power turbine inlet were 6- to 7-percent lower than those of the test engine.

Transient operation was validated by comparison to DISCUS-generated time histories. The control system was disconnected so that transients resulting from direct fuel-flow inputs could be compared. Under these conditions, large changes of fuel flow result in large changes of power turbine speed. Power turbine efficiency is modeled as a function of its speed in the real-time model only for small speed excursions about the design point. Transient data were therefore received from executions of the manufacturer's program with the power turbine dynamics suppressed, allowing power turbine speed to be constant. Output torque was then used as a measure of engine power. Fuel inputs were applied as instantaneous steps.

Results are illustrated in figures 10 and 11. As shown in figure 10, the two simulations are in close agreement for a step increase from midpower to high power. Gas generator speed was overestimated by approximately 2 percent. This overestimation was due mainly to performance map approximations, whereas the output torque responses correlate well. Power turbine inlet temperature was underestimated by the real-time program. The model experienced this discrepancy under all validation conditions. Because the error is small and dynamic characteristics are retained, the modeling of power turbine temperature is considered adequate. Low-power engine performance is shown in figure 11, which represents a step decrease in fuel flow to below idle power. The real-time model torque again shows close agreement with DISCUS. Gas generator dynamics are also accurately modeled.

An example of the closed-loop engine performance with a blade-element helicopter simulation is shown in figure 12. Flight test data obtained from reference 18 were used as inputs to the real-time program and test results are included for comparison. Turbine speeds and torque output are reproduced correctly. Discrepancies seen in fuel flow are attributed to the type of sensor used on the test vehicle. This sensor was mounted upstream of the HMU's sensor and therefore did not correctly reproduce the fuel-flow transients.

Generic Mission Tasks

A list was composed of simple segments of maneuvers that could be reasonably and simply simulated on MGH and that would highlight the advantages of an integrated flight and propulsion control system. The list was based on past

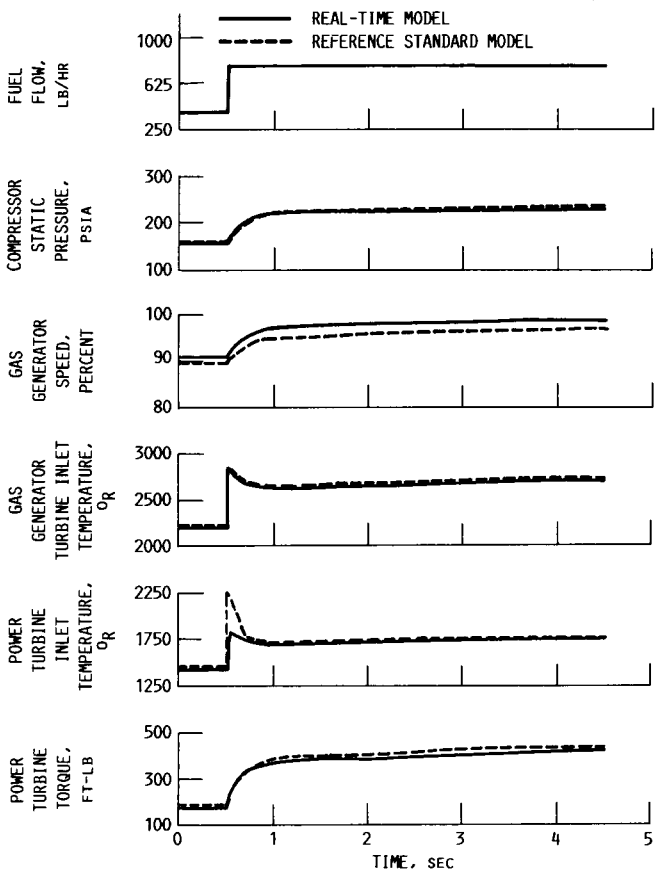

Figure 10.—Step fuel-flow increase from midpower to high power.

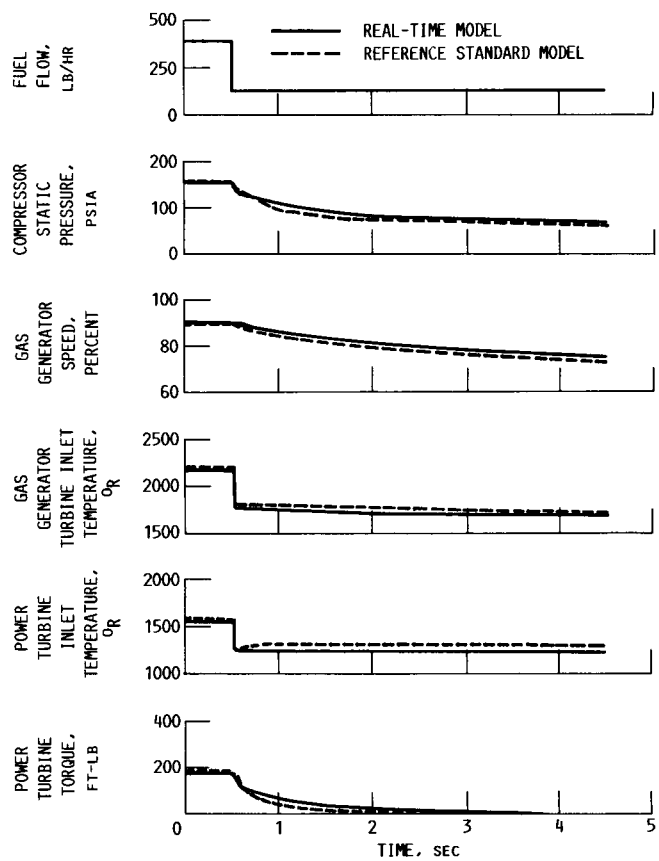

Figure 11.—Step fuel-flow decrease from midpower to low power.

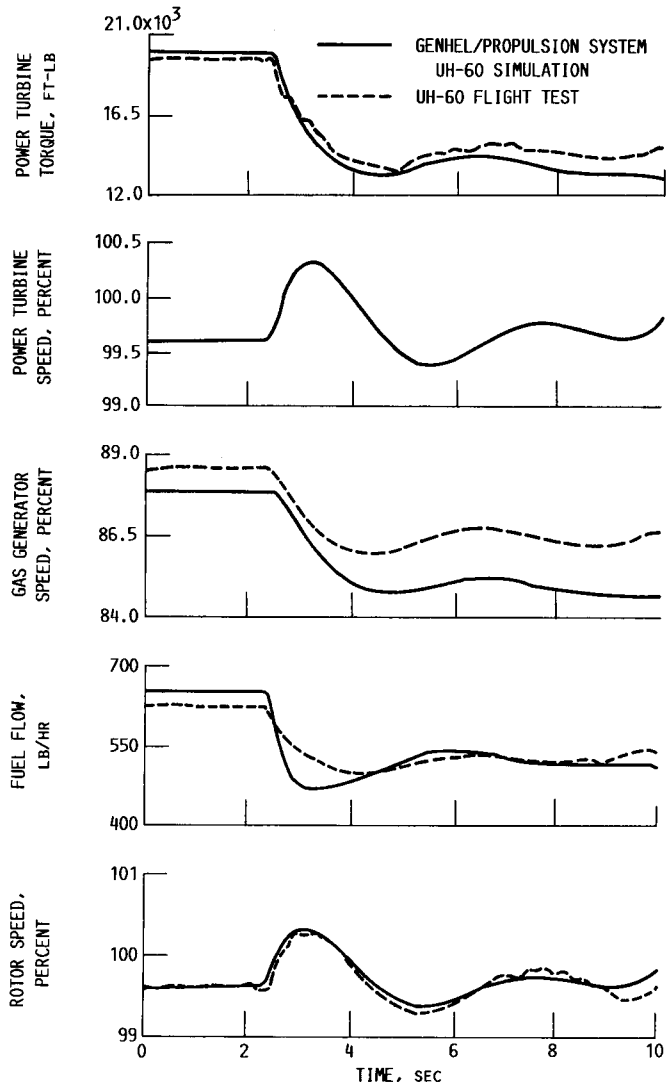

Figure 12.—Propulsion system response when used in conjunction with real-time rotorcraft simulation (10-percent-down collective input, 60 kn indicated airspeed).

experience of helicopter design problems and on a search of the AACT data base. Maneuvers were sought that entailed rapid changes in torque loading on the main rotor because this is the area where flight-propulsion control integration schemes are likely to be useful. The typical control problem is that during a maneuver in which the main-rotor torque load changes rapidly the engine is unlikely to be able to respond quickly enough to keep the rotor speed constant. Control power is a function of rotor speed squared; therefore, a 5-percent drop in rotor speed can cause a 10-percent change in stick sensitivity. This makes for great difficulties in precision flying. In extreme cases of autorotational recoveries, drops of 15 percent have been recorded. Although precision maneuvering may not be required, maintaining even a loose flight profile is difficult.

A list was composed as the result of reviewing past design experience and searching the AACT data base. The resulting list includes classic autorotative recovery, bob-up and remask, quickstop and quickturn deceleration, engine failures, side accelerations, and roll reversals. Most of the results were taken from the AACT data and all of the data were on aircraft other than the Black Hawk. Because the Black Hawk is relatively benign in its flight behavior, a fact due mainly to its heavier rotor, it did not exhibit the type of flight data sought. So, to illustrate these problems, we obtained all of the data on aircraft other than the Black Hawk.

The first five items in the list resulted from gathering comments from pilots and designers at Sikorsky on the type of maneuvers discussed earlier and grouping them into maneuvers that they felt could be amenable to simulation on MGH using the maneuver controller as an input.

The recent U.S. Army AACT tests were performed by personnel from the Army Applied Technology Laboratory, the U.S. Navy Test Pilot School, and industry. Well-instrumented helicopters of various designs were flown at Patuxent River, and data were recorded. First the aircraft were flown individually through a list of prescribed aggressive maneuvers, (the Maneuver Criteria Evaluation Program (MCEP)), and secondly they were flown in pairs in simulated one-on-one air combat. The latter was in both loosely prescribed and free-form maneuvers in which each aircraft was alternately the aggressor, then defender.

The integrated-control study concentrated on maneuvers that exhibited a rotor speed excursion of more than 5 percent on any aircraft. All such maneuvers were then classified by type and further studied in an attempt to understand the underlying cause of the excursion and to assess whether it was configuration dependent or not. In this manner, the search and classification reaffirmed the significance of the first four items listed previously and added the side acceleration maneuver and the roll reversal maneuver. Details of these maneuvers are given in reference 15.

Integrated Flight-Propulsion Control Design

The following sections highlight each element of the integrated-control design concept and explain its purpose and the techniques used to integrate the feature into the overall system. Because the design is presently a computer simulation, no attempt was made to determine which part of the control software belongs on which processor or the optimal routing of signals between sensors, actuators, and processors. The majority of code is propulsion control oriented and, as such, fits comfortably into the fuel control module of the MGH simulation, with the exception of some unavoidable changes and additions. On an implemented design basis, one might expect to see more of the coding in a flight-controller processor and less in the engine processor. For example, the engine-failure detection logic is an obvious choice to remain with the engine, but subsequent actions to be taken could be expected to be placed in the flight controller. In the code developed for this study, all logic for the integrated control is situated in the

engine-control module. Memory requirements and execution speeds were not considered.

The core of the controller is an isochronous power turbine speed governor whose reference speed may be altered by various combinations of variables representing present or anticipated engine-airframe states. The power turbine governor itself consists of a linear-quadratic-regulator state-feedback algorithm in which rotor tip speed is estimated by a Kalman-Bucy filter. Additional adaptive logic is used to anticipate rotor decay and help recovery from the declutched state. The traditional collective pitch-to-load demand spindle input to the fuel control is retained, but in digital form. The equally traditional, collective pitch-to-tail rotor collective link is replaced by a measured engine torque-to-tail rotor collective link. An indication of power available to hover is provided for the pilot. A cue for inhibiting the application of collective input while the fuel control is on its acceleration schedule is provided by a logic signal. A variety of collective movements following engine failure, depending on height and velocity, are available. A switchable fuel-consumption minimizer operating in conjunction with added loops in the AFCS is also available.

Linear-quadratic-regulator power turbine speed governor.—The purpose of a power turbine governor for helicopter applications is to maintain constant power turbine speed in the presence of torque load changes in the helicopter rotor system. Such governors in the past have used feedback of the speed error from some reference value to regulate fuel flow to the engines. An early example of such a governor was the so-called droop governor, which allowed a speed droop of about 10 percent to generate enough error signal and, therefore, fuel flow to hold speed to a 100-percent reference value under high-load conditions and to 110 percent under no load. An improvement on this design, the addition of an integrator to the error loop so that the steady-state error could be removed, resulted in an isochronous governor that maintained speed at the reference value under all steady loads, transient loads not withstanding.

A limitation on this form of governor is caused by the existence of two torsional resonances in the drivetrain system. The resonances are caused physically by the engine and drivetrain rotational freedom working against the blade lag freedom across the blades lagging hinges. The torsional resonance of the main-rotor blades occurs at a frequency of the order of 2.7 Hz with the blade torsional resonance of the tail rotor at about 7 Hz. Hydraulic lag dampers are provided across the main-rotor hinges to add damping to the system. The damping is determined by ground resonance conditions rather than pure first torsional conditions. To avoid exciting these modes, power turbine speed governors have employed bandwidth-limiting designs that cut off considerably below the first torsional frequency. This feature limits the response of the engine and fuel control, resulting in control too loose to allow tight aircraft response during rotor torque load-changing maneuvers. It should be emphasized that the rotor load change referred to is a torque loading change and not a rotor thrust change. While a change in rotor thrust almost always results in a change in rotor torque load, the reverse is not true; the rotor may be supporting the aircraft in flight under maximum power conditions or in zero power conditions. In either case, the total rotor thrust is very similar but the torque loads are quite different.

The advent of all-digital controls has made the proportional-plus-integral governor easier to implement and has opened the door to more sophisticated mathematical techniques for overcoming the torsional mode problem. Use of higher order notch filters to attenuate response at the first torsional frequency have been implemented successfully (ref. 24). General Electric's approach in this study is to employ a linear-quadratic-regulator design that allows the bandwidth to be increased and thus improve the response time of the system. It has the additional advantage that the design can be optimized in any direction desired by the manipulation of a cost function.

General Electric provided a high-performance power turbine speed governor designed for the T700 engine coupled to an advanced, articulated Black Hawk helicopter rotor system. Modern control-system design techniques were used to obtain a higher bandwidth system than previously achievable through classic methods. The linear-quadratic-regulator (LQR) technique was used to design the governor, and a Kalman filter was included in the control system to estimate the helicopter main-rotor-blade velocity as one of the states in the design (ref. 11). The effect of the LQR governor in the frequency domain is to attenuate the resonant peak caused by the interaction of the helicopter main rotor and the power turbine. The LQR governor provides adequate phase and gain margin for good stability and robustness. The resonant peak attenuation combined with large phase margin allows the system gain to be higher and results in the increased bandwidth.

In summary, the control acts as follows. The LQR governor regulates power turbine speed by summing the product of calculated gains and system states. The system states characterize the dynamics of interest at every time segment. There exists one state for each independent energy storage element. The LQR gains are calculated from a linear state-space model of the engine and helicopter rotor system. This model is a system of first-order differential equations that are functions of the state variables and the inputs. The LQR is designed as though all the states are measured. The helicopter main-rotor-blade angular velocity cannot be measured in flight and is estimated using a Kalman filter observer. This observer is a closed-loop system that contains a simplified linear model of the helicopter rotor system. The Kalman filter design parallels the LQR design. The estimated rotor blade angular velocity is used in place of a measured value with no change in the

LQR gains. The resulting governor has a bandwidth of about 6 rad/sec compared to a bandwidth of about 3 rad/sec for current controllers.

The LQR design method as applied to the T700 fuel control uses a five-state model to represent the system (fig. 13). Average tip velocity of a main-rotor blade (NMR) and the main-rotor torque transmitted across a flap-lag hinge combination (QMR) are rotor states that cannot be measured directly. NMR is an approximation to the average blade-tip velocity which should reflect a change in torque loading better than shaft speed since the aerodynamic loads are a function of the former. Since NMR is a variable outboard of the lagging hinge, it cannot be measured directly without substantial instrumentation. In its place, a closed-loop system containing a model of this rotor velocity is used to estimate it. This system is called an observer and is designed separately from the main LQR governor loop.

A schematic of the observer is shown in figure 14. The observer system must meet the usual requirements of stability and performance with the added requirement that it calculate the estimated states of interest fast enough that the performance of the main loop is not affected. If the model of the system used in the observer is observable, all of its poles can be placed arbitrarily in the s-plane, with the restriction that complex poles be placed as complex conjugate pairs. Main-rotor-blade velocity is observable in the T700 system from power turbine speed. The Kalman filter algorithm places the system poles in a specific manner.

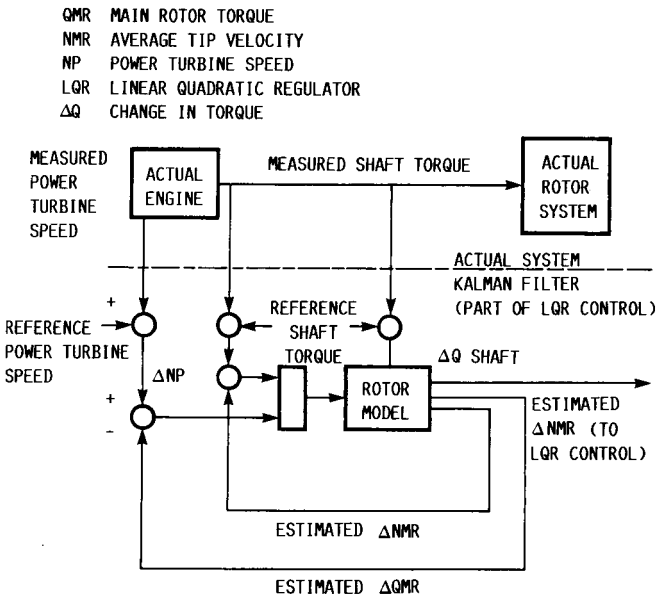

Figure 14.—Schematic diagram of observer.

The rotor model used for the observer is the simplified model shown in figure 15. The model neglects tail-rotor dynamics and the power turbine inertia is not lumped as part of the transmission as is done for the complete engine and rotor system. The rotor model is represented in standard state-space form. As previously mentioned, the states for this model are

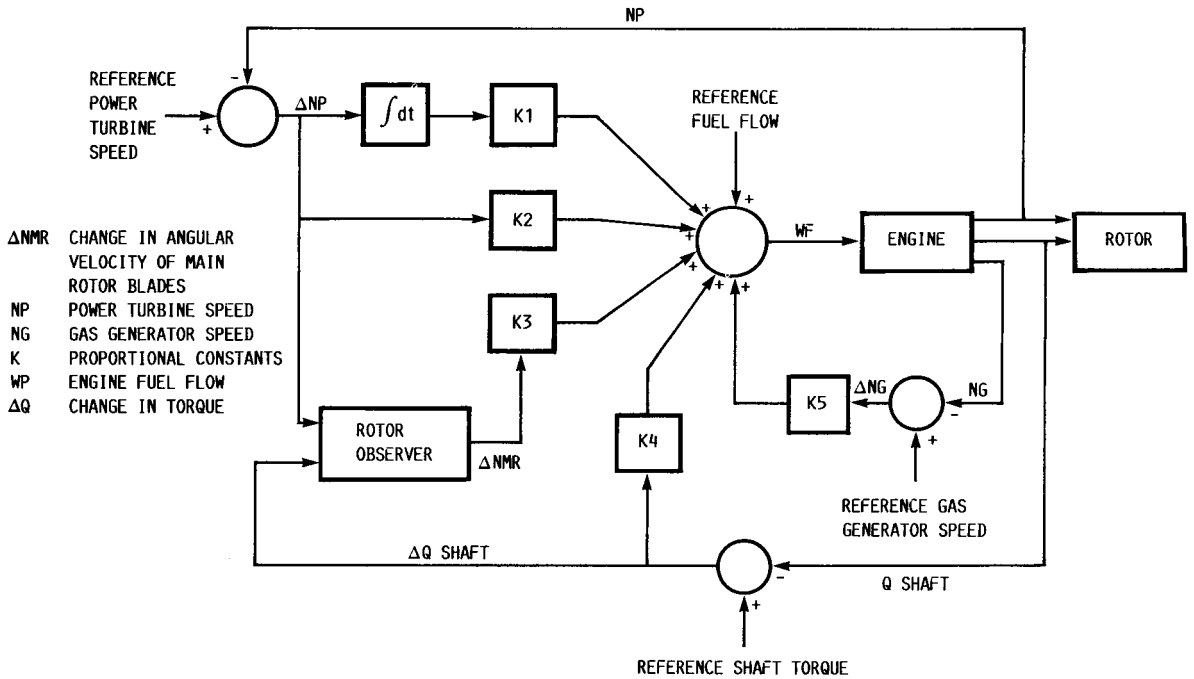

Figure 13.—Block diagram of engine and helicopter with linear state feedback.

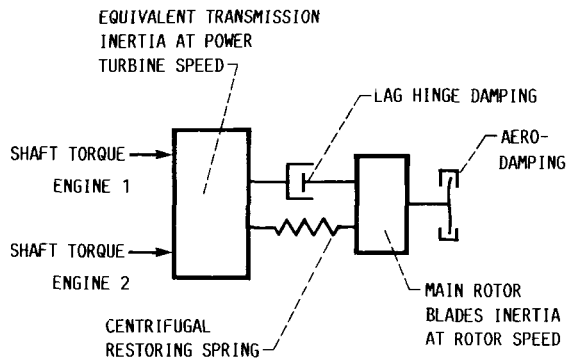

Figure 15.—Simplified linear helicopter model used in observer design.

main-rotor-blade average tip velocity (NMR), a main-rotor torque state (QMR), and power turbine speed (NP). The power turbine speed is used to approximate the transmission speed because the coupling between the power turbine and transmission is assumed rigid.

The LQR governor was analyzed in the frequency domain using standard Bode plot techniques to determine the system stability margins, speed of response, and disturbance rejection characteristics. These techniques are valid since the final LQR design is single input, single output. As shown in figure 13, the loop was broken at the engine fuel input to effect the primary stability analysis. A sinusoidal fuel-flow signal was input to the engine model at this point and the resulting fuel-flow feedback was measured at the output of the summing junction. This point in the loop is important because fuel flow is the main driver of the engine and it is also affected by all the engine states by the definition of full-state feedback. Fuel flow is also affected by the Kalman filter. The governor is a regulator that functions to reject disturbances to the power turbine. The controller reacts to these disturbances through fuel flow when they appear in the power turbine speed or shaft torque. In the frequency domain, the magnitude of the open-loop transfer function at fuel flow should be as large as possible over the frequency range where the disturbances occur so that they will be attenuated more effectively.

The system closed-loop frequency response was calculated for sinusoidal inputs at the gas generator speed, shaft torque, and power turbine speed sensors to determine the noise-rejection characteristics of the system. The disturbance-rejection characteristics of the system were analyzed by inputting a sinusoidal torque disturbance to the closed-loop system through the helicopter main and tail rotors.

As mentioned, the power turbine governor is a regulator that maintains constant power turbine speed in the presence of disturbances. The primary sources of disturbances are the helicopter main and tail rotors. The frequency response of the closed-loop LQR and T700 baseline systems was calculated for a main-rotor torque disturbance and a tail-rotor torque disturbance to analyze their effects on power turbine speed and helicopter main-rotor speed. The simulated disturbance was a sine-wave frequency sweep. Each disturbance was input separately. The response of power turbine speed to a main-rotor disturbance is shown for the LQR governor and for the T700 baseline governor in figure 16. The figure shows that disturbances are rejected better by the LQR power turbine speed governor than by the T700 baseline governor. This better attenuation of disturbances is also seen in time response traces. The helicopter main-rotor centrifugal spring constant can be considered proportional to the square of the main-rotor speed. From steady-state operation, this variable was considered a constant because rotor speed is governed at 100-percent speed. During a transient, however, the rotor will deviate from this design point and the centrifugal spring constant will vary as a result. To assure that stability margins are maintained at extreme variations from 100 percent, the spring constant was varied up and down corresponding to a ± 10 percent change in helicopter rotor speed. The spring constant is proportional to speed squared; therefore, the constant was increased 21 percent and decreased 19 percent. The frequency response results for increased and decreased spring constants showed that the system remains stable under both extremes.

The frequency response of the LQR governor was calculated with only one engine driving the helicopter rotor system (simulating the loss of one engine). Stability was not adversely affected but the bandwidth of the system was lowered from about 8 to 10 rad/sec to about 5 rad/sec.

The LQR governor did not attenuate the main-rotor resonance peak when the lag-hinge damping was reduced to zero. The frequency response of the system with zero lag-hinge damping was computed. The Bode plot, not shown here, shows that the system will not be stable for zero lag-hinge damping. Performance degradation and instability could result from this situation. It is possible, however, that an LQR governor could be designed to perform under this condition as well as in the normal damping situation.

Transient simulations of the engine with the LQR controller showed that the system was stable as predicted without the heat sink model, but unstable when the heat sink model was included. The heat sink model accounts for the effects of heat absorption by the engine metal mass during bursts and chops. Analysis of the heat sink model revealed that it contributed 25° of phase lag and 4.5 dB attenuation at 4 rad/sec. This lag, combined with other lags which were not accounted for in the design model, was sufficient to drive the system unstable. Comparisons of the frequency domain effects of this heat sink model with the effects of other similar models indicates that this phase lag is excessive. A lead compensator was added to the fuel flow output of the LQR controller to restore sufficient stability margins. This lead had a minimal effect on performance when the heat sink model was not included in the transient simulations.

The higher bandwidth translates directly into better performance in the time domain. The first transient considered is a simulated wind gust of 40 ft/sec over a distance of 200 ft, which causes a load disturbance in the rotor system. The LQR power turbine speed governor reduces the speed droop from

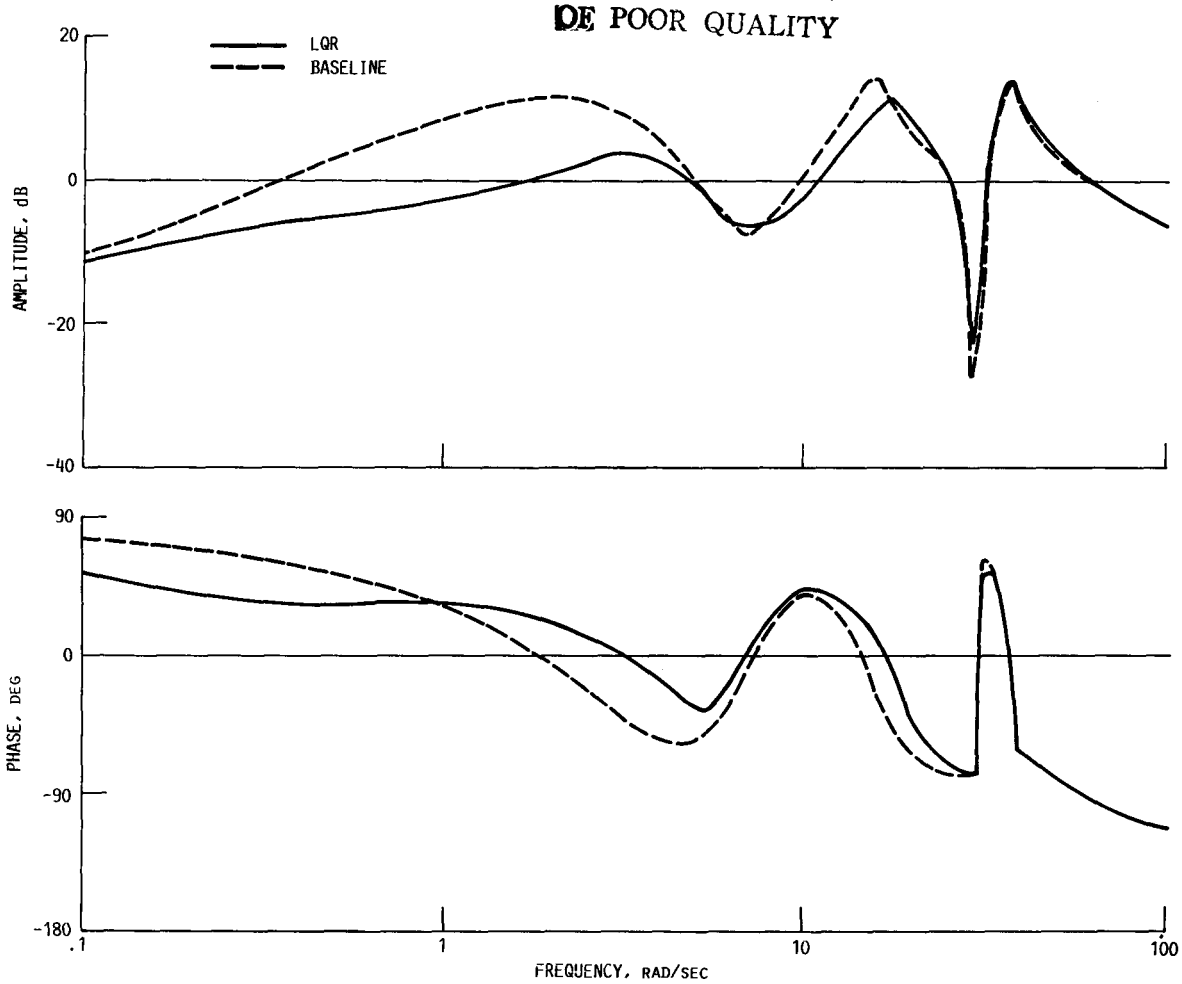

Figure 16.—Bode plot of baseline and linear-quadratic-regulator (LQR) power turbine speed response to main-rotor torque.

3.25 to 1.3 percent—a 60-percent reduction (fig. 17). The specific wind gust selected ends with gas generator speed at 87 percent, the point of minimum system stability margin. This effect is most evident in the rate of change of power turbine speed. The baseline control has several small oscillations before the system stabilizes. The LQR governor virtually eliminates these oscillations demonstrating its better phase margin.

Two additional transients are also shown demonstrating the responsiveness of the LQR power turbine speed governor. During both of these transients, the other integrated control functions that can affect system response either are not invoked or have been disabled to eliminate masking of the LQR response. Figures 18 and 19 show a roll reversal and a high-g turn, respectively. In both cases the power turbine speed is held closer to 100 percent with the LQR control. It is also noted that fuel flow varies over a smaller range thus indicating that the LQR governor makes better dynamic use of energy.

Pragmatic adaptive elements.—The adaptive fuel control designed and currently under development by Chandler Evans is fully described in references 12 and 25. The term "adaptive" has a variety of specific meanings but usually implies that the

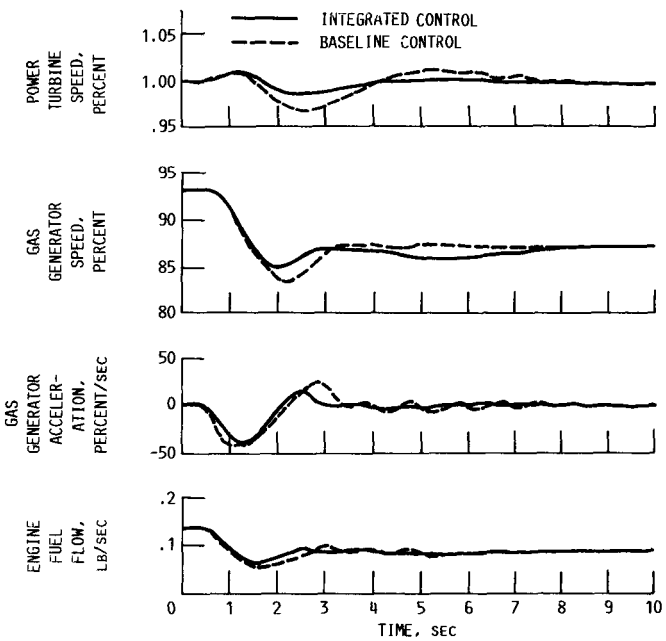

Figure 17.—Simulated discrete gust response using linear-quadratic-regulator (LQR) controller.

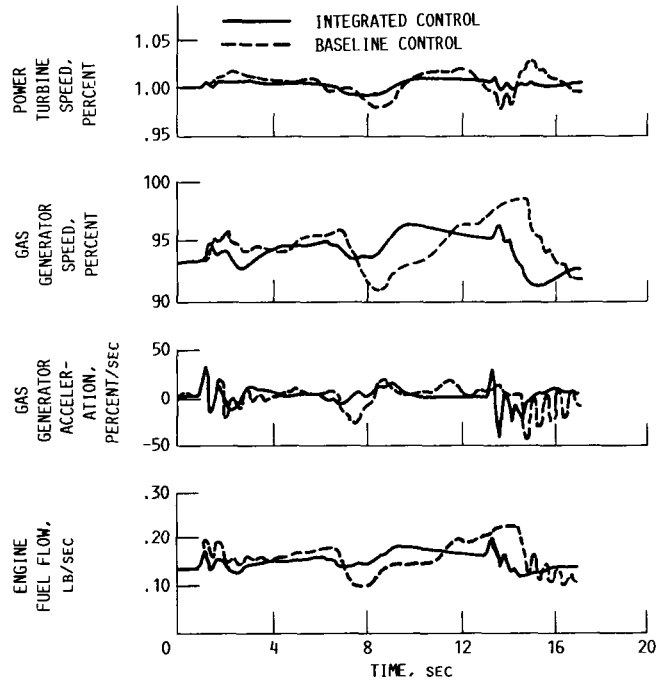

Figure 18.—Simulated roll reversal using linear-quadratic-regulator (LQR) controller.

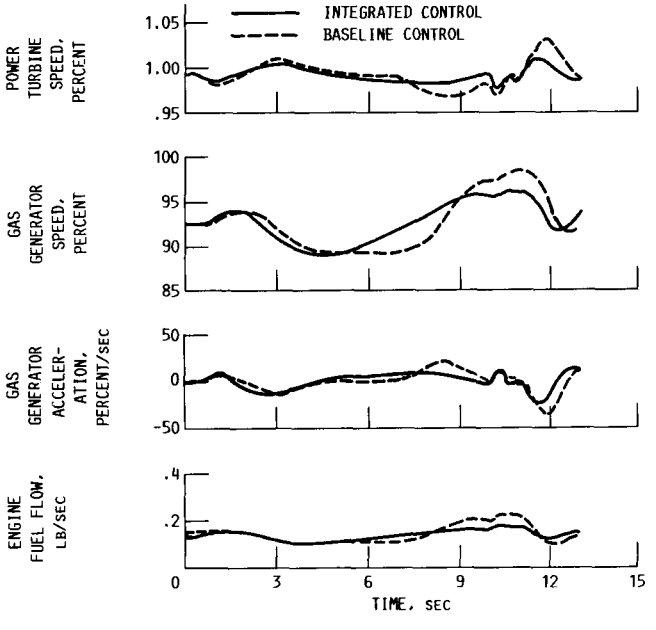

Figure 19.—Simulated high-g turn using linear-quadratic-regulator (LQR) controller.

system is capable of accommodating environmental changes that arise within the system or external to it. Adaptation is a fundamental characteristic of nature since it attempts to maintain physical equilibrium in the face of changing environmental conditions. There are different definitions of adaptive control systems now in use in the control world, and the vagueness surrounding most of them revolves around the failure to differentiate between the external effects of adaptation and the internal processes used to achieve it. To be called an adaptive system, the system must include self-organizing features. If the system parameters are adjusted by only direct measurement of the environment, then the system is not truly adaptive. In this sense, then, the adaptive features considered here are not adaptive classically but only pragmatically. To distinguish their behavior from a controller designed using the adaptive control, we refer to concepts of modern control theory as pragmatic adaptive control elements. Chandler Evans' controller recognizes an off-design condition in a practical way and compensates for it by using a prescribed logic decision set. It is not a linear system algorithm.

Figure 20 shows a block diagram of the integrated control which includes the LQR governor, the gas generator acceleration governor (NDOT governor), and the adaptive elements. The fuel-flow features of the control, other than the LQR governor, are derived from the pragmatic adaptive system.

The integrated control nominally operates on the LQR power turbine governor. In extreme maneuvers, it will be limited on the top end by the NDOT governor and on the low end by the bottom governor and NDOT deceleration limiter. On each cycle of the control computer, these limits determine the upper and lower extremes of the allowable fuel flow.

The structure of the integrated control is more complicated than that of the adaptive control as it involves three integrators: the LQR governor, the acceleration limiter, and the deceleration limiter. Reset logic was designed so that the integrators not in the winning path would not wind-up. The reset logic calculates backward through the control modes using the winning fuel-flow value. The nonwinning integrator values are reset as if they had produced the winning fuel flow. In this manner, the fuel-flow limits will always be appropriate for the current fuel flow and mode changes will be effected smoothly.

The adaptive features that affected the power turbine set speed in the adaptive control system are applied to the LQR power turbine speed setpoint. These features included torque sharing, rotor decay anticipation, rotor droop recovery, and load factor enhancement. Collective rate anticipation was not included since the LQR governor had its own collective-pitch maps.

The LQR governor is essentially a small disturbance device. In particular, it was not designed to handle a decoupled rotor system and the pragmatic adaptive control elements have to deal with such situations. For the autorotational rotor decay anticipation, the adaptive control provides a flag that signals when the system goes into autorotation. This flag is set by comparing the power turbine speed and the rotor shaft speed. When the difference is greater than a deadband, the flag is set. This flag is used by the LQR governor to decrease the gain in its loop tenfold and to switch out the rotor tip speed, shaft torque, and core speed paths. These paths add no information to the LQR in autorotation, and it is temporarily

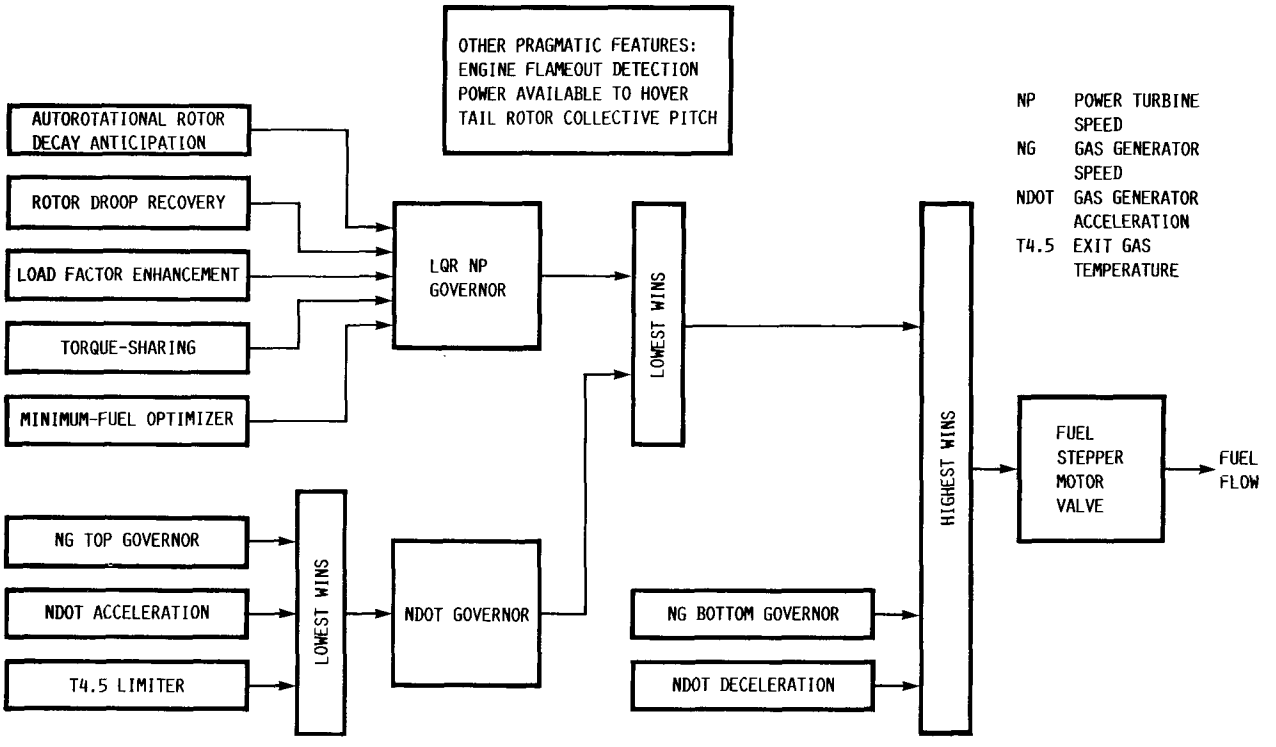

Figure 20.—Block diagram of integrated control.

converted into a proportional-plus-integral controller with a low gain.

The autorotational rotor decay anticipator, acting on the autorotation flag, generates an incremental power turbine speed reference to the LQR controller to keep the power turbine at a higher acceleration potential so that engagement of the engine and rotor will occur at a higher engine speed and presumably reduce droop. The effect of this control element is discussed later in the evaluation section.

The logic of the droop compensator subsystem is to detect that a droop has occurred and to inhibit the likely torque and subsequent speed overshoot that will follow. This is accomplished by deliberately delaying the governor-demanded fuel flow. As the droop starts to diminish, a signal is generated that reduces the power turbine speed reference, thus, reducing torque load and speed overshoot.

The acceleration schedule is the usual control that seeks to inhibit compressor surge by allowing the gas generator to accelerate in a preprogrammed fashion with maximum acceleration as a function of gas generator speed. Chandler Evans has incorporated their adaptive surge margin compensation and also used a lagged compressor discharge pressure to further stabilize surge recovery.

The gas generator topping-speed action simulates the action of the pilot controller power available spindle by acting as an upper-limit throttle on gas generator speed and, thus, on maximum engine power output. The purpose of this limiter on the original T700 fuel control is to give the pilot some control if the electronic function should fail. Its retention here gives similar control, but the failure mode that would warrant its use has not been fully determined. In any case, it does serve as an absolute gas generator speed limit.

The temperature-limiting section is a straight-forward digital implementation of a power turbine inlet temperature limiter. A logic switch, which is triggered by the engine-failed status flag of the other engine in a twin-engine installation, can boost the allowable temperature for emergency power situations.

The lowest output of the these three governor sections is passed to the NDOT governor section, which produces an error signal from the difference between its integrated value and the sampled gas generator speed value, calculates a weighted proportional-plus-integral gain, and multiplies this gain by lagged compressor discharge pressure. The resulting fuel flow is the gas generator fuel flow that is compared to the power turbine speed governor flow on a lowest-wins basis. The three components of the gas generator speed governor thus serve as alternate top limits to the fuel flow. The integration in this governor is back-calculated when the top limits are not being applied to the value corresponding to the actual fuel-flow value selected by the complete system and to the gas generator acceleration value measured at the corresponding time. Thus, any transition into the limits is smoothly negotiated by the integrator.

A prescribed deceleration schedule is provided to ensure sufficient margin from compressor stall. This path contains an integrator that is controlled by back-calculation in the same way as the NDOT governor while the deceleration control is not governing the fuel flow.

A bottoming governor, which prevents the gas generator speed from falling below a prescribed self-sustaining lower limit, is also supplied.

The last two flow limits are compared on a highest-wins basis with the power turbine speed governor demand. The resulting fuel flow is the demanded fuel-flow value that is passed to the stepper motor, which regulates very precisely the pumping of fuel into the engine. A power-turbine-speed-actuated overspeed switch cut-off value is present on the engine side of the stepper motor to deal with runaways such as shaft failures.

Thus, the fuel flow delivered by the controller to the engine via a stepper motor is subjected to various limitations from other parts of the controller. On increased power demand, the power turbine speed governor fuel-flow requirement may be limited by the lowest of three limit governors: (1) the gas turbine speed topping limit—a variable which protects the engine by limiting the speed of the gas generator part as a function of the power-available lever angle chosen by the pilot, (2) a gas generator acceleration limiter with built-in adaptability to avoid compressor surge and stall after a first occurrence, and (3) an engine power turbine inlet-temperature limiter. If the lowest fuel flow from any of these three governors is lower than that of the power turbine speed governor, it is given precedence.

On decreasing power demand, the engine is protected by two other limit governors: (1) a gas generator bottom limit—a low-fuel-flow limit that is a function of ambient temperature and the compressor state and (2) a gas-generator deceleration limit—a maximum deceleration rate for the gas generator. If the fuel flow from either of these two limiters is higher than that from the power turbine speed governor, it is given precedence.

After these limits have been applied, an overall maximum and minimum fuel-flow limitation is imposed, followed by a final power turbine overspeed shutoff.

Three other subsystems can influence the fuel flow by changing the power turbine speed reference signal in the power turbine speed governor. The first is a dual-installation torque-sharing device that is the digital equivalent of the baseline T700 controller. This controller indirectly speeds up the gas generator of the low-torque engine to match the output of the nondegraded engine by applying to the lower engine an incremental power turbine speed reference signal that is proportional to the torque error.

The second subsystem is the minimum-fuel-consumption optimizer. This is an extremely simple algorithm that, when switched on in cruise, samples the fuel flow at intervals and perturbs the power turbine speed reference signal to change the rotor speed. Once the required direction of rotor speed is established, the system makes successively smaller changes until either the authority limit is reached or small changes about the optimum value are continually made. This is an extremely long term action with a time constant measured in minutes rather than seconds because of the long soak times taken by the engine before settling down. The flight control system of the simulated Black Hawk had to be modified for this system. Figure 21 shows the results achieved by the simulated MGH Black Hawk system. Since the attitude hold was inappropriate, it was switched off and an altitude hold was introduced in its place. The airspeed hold outer-loop flight path stabilization action was retained, thus allowing the FPS to counter the trim changes induced by changing rotor speed and to maintain a trimmed flight path. Because of the effect of rotor speed on control power, there is room for improvement in the FPS gain selection when performing these duties.

The third subsystem is the load factor enhancement feature. In general, it is possible to increase the aerodynamic load factor capability of a helicopter by increasing the rotor speed. If the local blade incidence angle is in stall, the increase in speed may reduce it to below stall and the increased total head pressure will produce more lift. If the rotor is power limited, the decrease in the incidence angle and hence drag coefficient may allow the increased lift to be obtained for almost no power increase. However, at high speeds, where the drag coefficient is largely a Mach-number-dependent phenomena, this is no longer true. Figure 22 shows the order of magnitude of the effect as predicted by the MGH simulation. A simple increase in rotor speed reference was conceived as part of the original pragmatic adaptive controller, which would be triggered on

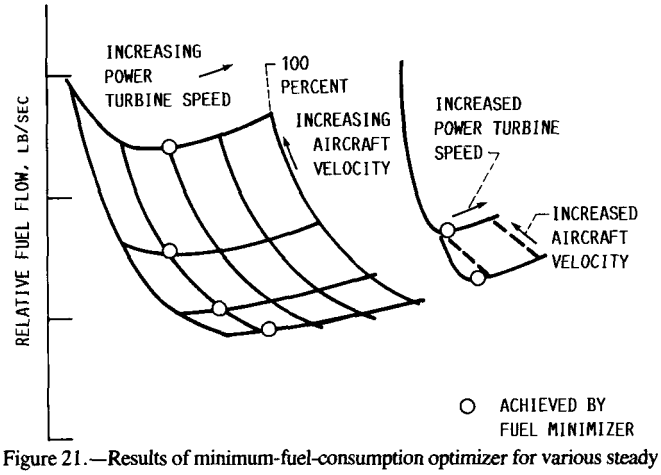

Figure 21.—Results of minimum-fuel-consumption optimizer for various steady cruise aircraft operating conditions of the MGH Black Hawk simulation.

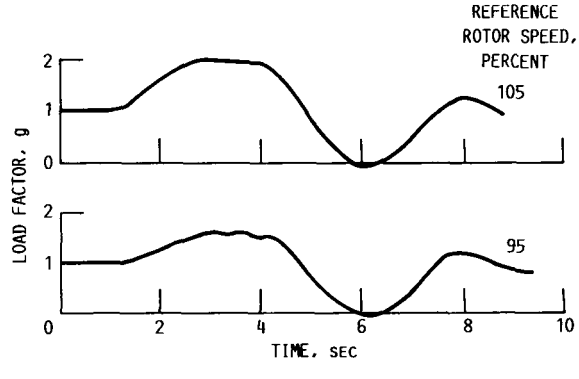

Figure 22.—Effect of load factor enhancement feature during pull-up maneuver.

load factor above a threshold value while being proportional to load factor with overlapping switching steps to prevent ratcheting. Because the load factor signal was very noisy, ratcheting did occur in the simulation. Even with smoothing, the changes in the power turbine speed looked far too abrupt to be anything but unsettling to a pilot. The final form of this subsystem involved ramping an increment in rotor speed reference proportional to dynamic head and keeping it on for some time after the load factor was removed. This procedure tends to keep the engine spooled up for a longer time and, thus, able to deal better with large torque increases should the rotor pop in and out of an autorotative state. This is one area where it became rapidly apparent that a pilot-in-the-loop evaluation is essential.

Other pragmatic adaptive features.—The flame-out detector relies on the accuracy and constancy of the relationships between a gas generator deceleration and the gas generator speed at which flame-out occurs and the range of gas generator decelerations at normal, operating gas generator speeds. Figure 23 shows the relationships of the normal decelerations being limited at various gas generator speeds by the governor's minimum fuel-flow limit and fuel-valve slew rate limit. The detection boundary is the line that appears to give adequate clearance to avoid false signals at legitimate gas generator decelerations while giving as much warning as possible. The logic failure signal is arranged to give a visual warning in the cockpit and may initiate other actions also.

The power-available-to-hover computation uses nominal maps of corrected engine torque and power turbine inlet temperature to calculate the maximum torque available from the engine. These maps are continually updated to include any engine degradation. The engine deterioration is stored into the computer memory by modifiers of these maps. Thus, maximum torque available is diminished if engine performance is degraded. The torque required to hover is calculated from a map of the ratio of hover-torque required to current cruise torque versus airspeed as shown graphically in figure 24. While the helicopter loiters at constant airspeed, the current torque is used to determine the torque required to hover for the current conditions. Gross weight, wind direction, and altitude are not directly involved in the calculation. Maximum torque available (PAH) is then compared to torque required to hover (PRQ). A positive difference indicates spare torque and a hover is therefore feasible.

Figure 25 shows the kind of indicator that might be provided in the cockpit. The power-available (PAH) pointers move up and down the outside of the engine-torque ribbon percent indicators. The power-required (PRQ) pointer moves up and down between the two ribbons. It is illuminated in red when

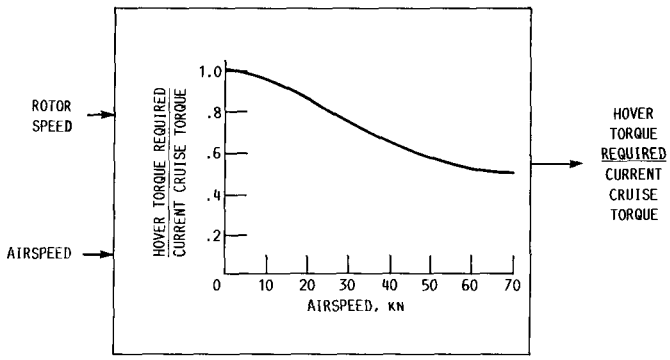

Figure 24.—Predicted torque required to hover ratioed to cruise operating torque.

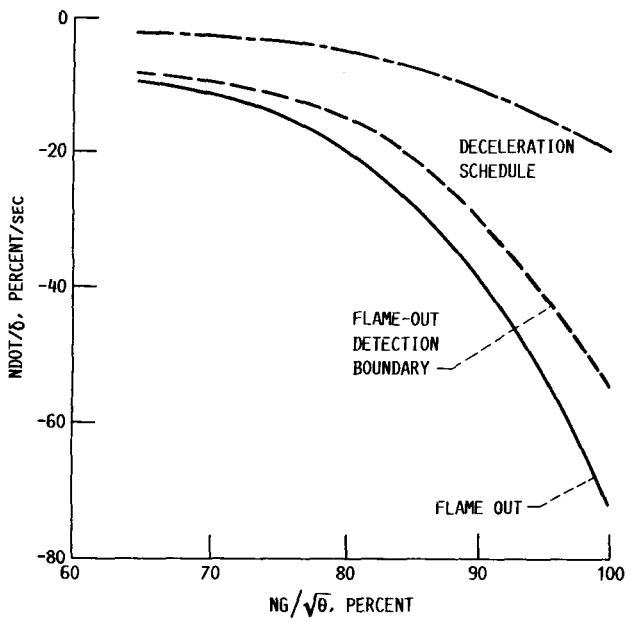

Figure 23.—Flame-out and normal engine deceleration rates.

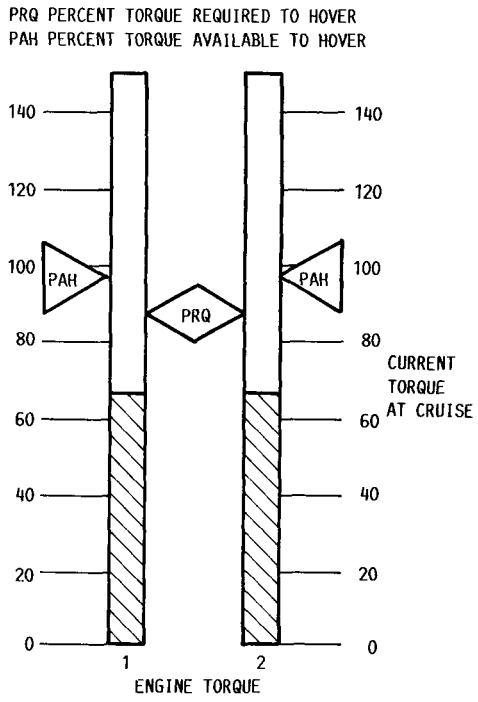

Figure 25.—Power available to hover indicator for dual-engine configuration.

above the power-available indicators and green when below. At airspeeds above 50 kn, the illumination of all three pointers is turned off.

Airframe-originated features.—As mentioned briefly in a previous statement, the collective pitch-to-tail rotor collective link has been removed in the integrated control in favor of a sum of engine output torques to tail-rotor collective link. In maneuvering situations, where the torque load on a rotor can change very quickly as the attitude and airspeed change, collective pitch becomes a misleading guide to the rotor torque load and thus also to the compensation required in the yaw axis. The ideal link would be one that produces a yawing moment proportional to the main shaft torque load. Unfortunately, the shaft torque is very difficult to measure and the production of yawing moment via manipulation of a tail-rotor collective pitch mechanism is far from linear, making the proportionality property equally difficult to achieve. The integrated control solution is to use the sum of the engine output torques as an approximation to the main rotor shaft torque and to live with the nonlinearities inherent in the tail-rotor collective yaw controls. Another alternative, which is outside the scope of this study, is to consider model-following control laws wherein rotor torque is modeled in a nonlinear mode and included in the control system in closed-loop fashion.

The analytical gearing of this linkage was chosen to yield pedal trim positions similar to the present Black Hawk baseline controls. Figure 26 is an example of the trim positions through the speed range at a fairly light weight. An exhaustive investigation of the trim position and margins was not undertaken in this study. This linkage is destabilizing to the natural Dutch roll mode but not noticeably so with augmentation on.

Another feature programmed into the control is the use of the fuel-control status flag. This flag signals, in addition to all other control levels, that the engine is on its acceleration schedule and is increasing output torque at the highest rate possible. Thus, this flag can be used to inhibit the pilot from applying increasing torque loads via the collective pitch input faster than the engine can absorb these loads without allowing droop to occur. In the mechanization proposed here, the status

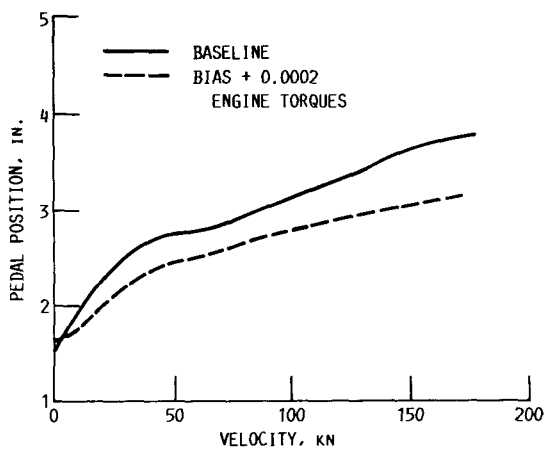

Figure 26.—Linking pedal position to sum of engine torques.

flag signals an electric clutch mechanism on the collective lever which adds about 12 lb of retardant stick force when the lever is moved in the upward, or torque-increasing, direction. The pilot can override this level of stick force somewhat easily if he feels it to be necessary under his particular flight condition. In use, a pilot would pull the collective-lever until he or she felt the force increase and then maintain a steady pressure that would allow the stick to step upward in very small increments as the controller switched rapidly on and off the acceleration schedule. The collective pitch control thus increases at an optimal rate constrained by constant rotor shaft speed. Figure 27 shows the response obtained in an autorotative recovery by simulating the pilot's collective-lever pull limiter with a simple integrator that is switched on and off by the status flag as it indicates being on the acceleration schedule. (The response to the same input without the inhibitor control is also shown in figure 29, which is discussed later in a different context.)

The framework for a torque spike response inhibitor was written when this phenomenon was first noted in the flight data survey. However, in all the cases which were run to exhibit the performance of the integrated control, the LQR power turbine speed governor on the Black Hawk dealt adequately with the roll reversal torque load thus indicating the effectiveness of this modern control concept. The extra compensation planned to be applied when bank angle was positive and roll rate was negative via the engine load demand spindle was not required, and further development was not pursued in this application. Nevertheless, the technique appears to be a valid approach to the problem and may produce positive

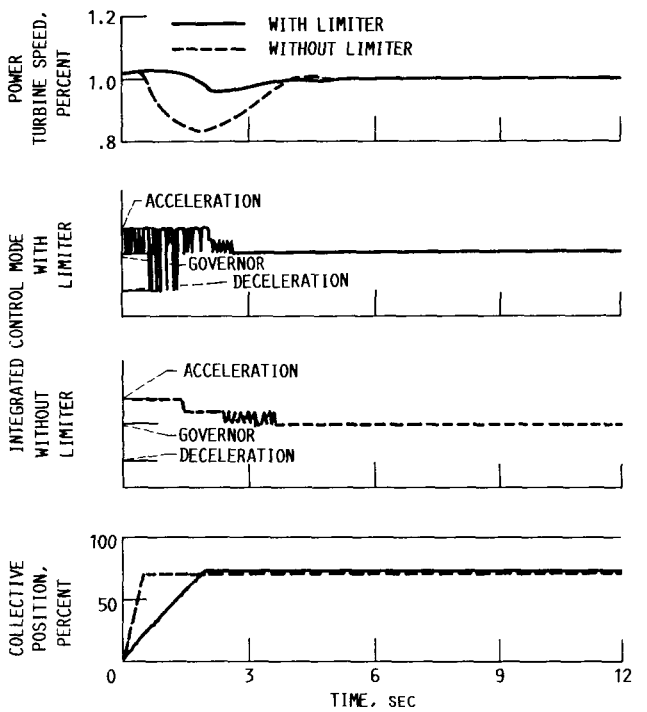

Figure 27.—Simulated autorotational recovery using collective-pitch-lever pull limiter on acceleration schedule.

results on other vehicles with control systems that do not use modern-control engine applications.

The last feature to be considered in airframe-originated, integrated control items is that of automatic control action required under single- or dual-engine failures. There are four separate facets of this problem, two at high speed and two at low speeds, or hover. Figure 28 illustrates the response of a modern helicopter to a dual-engine failure at high speed simulated by a dual throttle chop. The Black Hawk's response is not at all similar since the heavy rotor tends to keep the shaft speed higher and the large fin area, coupled with the more effective speed of the tail rotor, make the directional stability much greater. Hence, sideslip never develops and the roll response due to the dihedral effect is very mild. Since no problem existed on the Black Hawk and a change in rotor mass to provoke the effect would have a large impact throughout the integrated control design, no further studies were conducted. It seems quite possible, however, that, if needed, the engine flame-out warning flag could be used at higher airspeeds to impress a tail-rotor pitch input early enough to prevent the yaw and consequent roll response as seen in figure 28.

The other high-speed problem is merely that of low altitudes. In this case, the undercarriage must not be allowed to have ground contact above speeds consistent with its design considerations. To avoid this, the speed-altitude prohibition curves in the pilot's handbook include a forbidden zone of below 25 ft

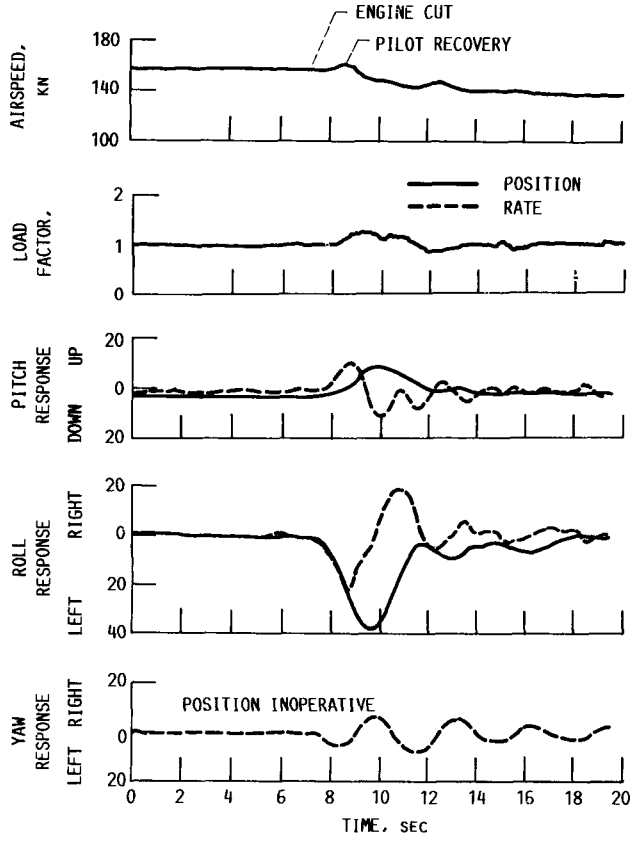

Figure 28.—Response of a modern helicopter to a dual-engine failure at high speed.

at all speeds higher than 55 kn. No automatic means of decreasing this area is envisaged. Although, for a machine designed primarily for NOE missions, the undercarriage would probably be strengthened sufficiently to move the prohibited area out to about 80 kn. The safe procedure in such circumstances is to flare the aircraft by pulling the nose up until enough speed is lost to make a safe landing. This is similar to a quickstop maneuver without the hover recovery portion.

The low-speed facets are the familiar deadman's curves listed in most pilot handbooks. At low speeds for given atmospheric conditions and gross weight, there are two critical altitudes beyond which, after an engine failure occurs and is recognized by the pilot and action taken, recovery is not possible. The lower limit altitude is that above which the vertical velocity cannot be reduced enough to prevent ground contact at above the critical rate for the undercarriage strength. The upper limit altitude is that below which the pilot cannot fly away on one engine without ground contact or, in the case of a dual failure, make a controlled autorotational descent and landing. A large part of the prohibited area is created by the requirement to allow the pilot time to recognize the problem and react to it. The automatic control envisioned would recognize the height-velocity area in which failures occurred and take appropriate action immediately on perceiving the failure flag.

The application of cyclic and collective would depend on the area of the altitude-velocity diagram where failure occurred. It would be preprogrammed or would possibly use the power-to-hover and performance mapping information of the pragmatic fuel controller to make logical decisions. The stick would be moved by clutch mechanisms that could be overridden by a pilot using stick force alone. The movement-causing forces would be faded out after several seconds. Pilot-in-the-loop simulation is the only way to assess such schemes.

Screened-out features.—A number of features were considered in addition to those presented above but were not included because of impracticability and modeling limitations. These included T700 inlet-guide-vane variable geometry, Dutch roll and torsional mode tuning, stabilator setting and fuel minimization, engine bleed, and engine surge avoidance. These features and the reasoning for not including them in this are study are presented in some detail in reference 15.

Control System Evaluation

The evaluation of the integrated flight and propulsion control was conducted in two phases. The first evaluation, presented here, was accomplished using the MGH simulation facilities at Sikorsky. The second part was to be a pilot-in-the-loop study on the NASA Ames VMS. The VMS evaluation has not yet been accomplished. However, a brief discussion on the program content is presented.

Evaluation using MGH.—The mission segment tasks listed previously were simulated using various control strategies including analytical inputs, flight-path profiles, and a

sophisticated partial model-following technique called a maneuver controller. The analytical input method consists of specifying input levels on any input variable as functions of time. Steps, pulses, doublets, and sinusoids are available including other arbitrary and analytical functions. This form of input is adequate for the simplest of maneuvers but does not fly the aircraft like a pilot.

The flight path profile technique is an improved method where flight path profiles are required to be flown. The profiles are specified as time histories and a control variable is assigned to control each one. This method is quite effective and was used for most of the maneuvers performed during this study. However, the flight path profile technique cannot cope well if appreciable cross-coupling is present, a condition that arises quite often in integrated-control studies.

The maneuver controller alleviates the cross-coupling problem and provides a means of flying a specified maneuver. The technique is a partial model-following system in which a flight-profile time history is specified and passes through a series of filters that shape a required vector of time-varying variables that would smoothly accomplish the required maneuver if flown by the helicopter. The controller is not capable of flying the more subtler aspects of maneuver techniques. Whichever piloting method was chosen for a particular maneuver, it was maintained as the control strategy for both the baseline and the integrated control cases. It proved extremely difficult to fly the aircraft anywhere near the aerodynamic boundaries because even the maneuver controllers could not adapt sufficiently to deal with the changes required of them in the course of flying the more complex maneuvers.

To optimize the ease of task accomplishment, a powerful paper pilot model would be required to thoroughly evaluate all aspects of both (1) the techniques required to fly a maneuver and (2) the control system characteristics. Knowing this, the MGH evaluation concentrated on flying each maneuver in as simple and repeatable a way as possible in order to make comparisons between the baseline and integrated systems. A complete and exhaustive evaluation of the the integrated control was left to the pilot-in-the-loop study where a human pilot responding to realistic visual, aural, and motion stimuli could be expected to make a more complete assessment.

The evaluation was performed by flying the simulation through a series of maneuvers. Each maneuver employs various items in the integrated control to different extents. Where the behavior is similar, it is not enlarged upon and reference is made to the first descriptive occurrence.

In general, the Black Hawk simulation was flown with the SAS and FPS off. Both subsystems could be expected to be incorporated in a total integrated control design. Flying with the SAS active is a way of acknowledging that incorporation. The FPS functions of the Black Hawk were largely inappropriate for this study. The force augmentation system is meaningless without piloted controls. The coordinated turn feature was provided by the input maneuver controller. Since leaving the FPS feature on caused interference with the controller operation, the simulation was flown with the FPS feature off. The attitude hold feature was the opposite of what was required for the fuel-minimization scheme.

Autorotational recoveries.—Figures 29 to 32 are the simulated autorotational recoveries for each of the four types discussed previously. The splits were 17 and 2 percent and the collective lever pull times were 3.0 and 0.5 sec. In each case, the collective pitch was pulled up to 70 percent, which resulted in a final climb rate of over 3000 ft/min from an initial descent rate of just under 3000 ft/min. The cases were flown by applying a ramped collective input while allowing the maneuver controller to act as a full authority rate damper in roll and yaw. Thus, the pedal activity necessary to counteract the large changes in main-rotor torque loading while keeping the yaw rate small can easily be seen and the two systems compared. The standard SAS was switched on. The solid lines on the figures indicate the integrated control and the dashed lines represent the baseline control.

Recovery with large split and slow pull: Figure 29 shows the recovery from a 17 percent split using a 3.0-sec collective pull on autorotative recovery. The rotor speed droop is reduced from 10.5 to 2 percent. The normal load factor is higher than the baseline by about 0.25g, a condition presumably due to both direct and indirect effects of the higher rotor speed. The direct effect is to produce more lift and the indirect effect is to produce more pitching moment, which allows the nose of the aircraft with the integrated control to move higher at an earlier time. The rate of climb reflects the increased lift between 2.0 and 8.0 sec. The amount of pedal and pedal reversal movement and the direction required to keep the rate of yaw small is seen to be less for the integrated control while the applied control at the tail rotor is much the same. It is not particularly clear from the power turbine output versus shaft speed plot, but it can be seen on the engine clutch state trace that the integrated controller causes the engine to engage with the main shaft earlier than the baseline controller does. This early engagement is due to the rotor decay signal producing a fuel flow to speed up the gas generator as well as the collective pitch link. Once engaged, the LQR governor takes over and detects that the power turbine is overspeeding and puts the controller onto its deceleration schedule by demanding a large decrease in fuel flow. Eventually, the power turbine speed governor requires short bursts on the acceleration schedule before it copes in its own range with a quite smooth recovery. In contrast, the baseline controller detects the gas generator overspeed caused by the load demand link and switches to its deceleration schedule before the clutch engages. Details of the baseline fuel demands are not plotted, but the net result of the cutback at the wrong time is a 10.5-percent droop in rotor speed.

The requested fuel flows in the different sections of the integrated control have all been reset by the integrator reset logic before sampling occurs. Therefore the selected fuel flow plots are used in determining the fuel control action.

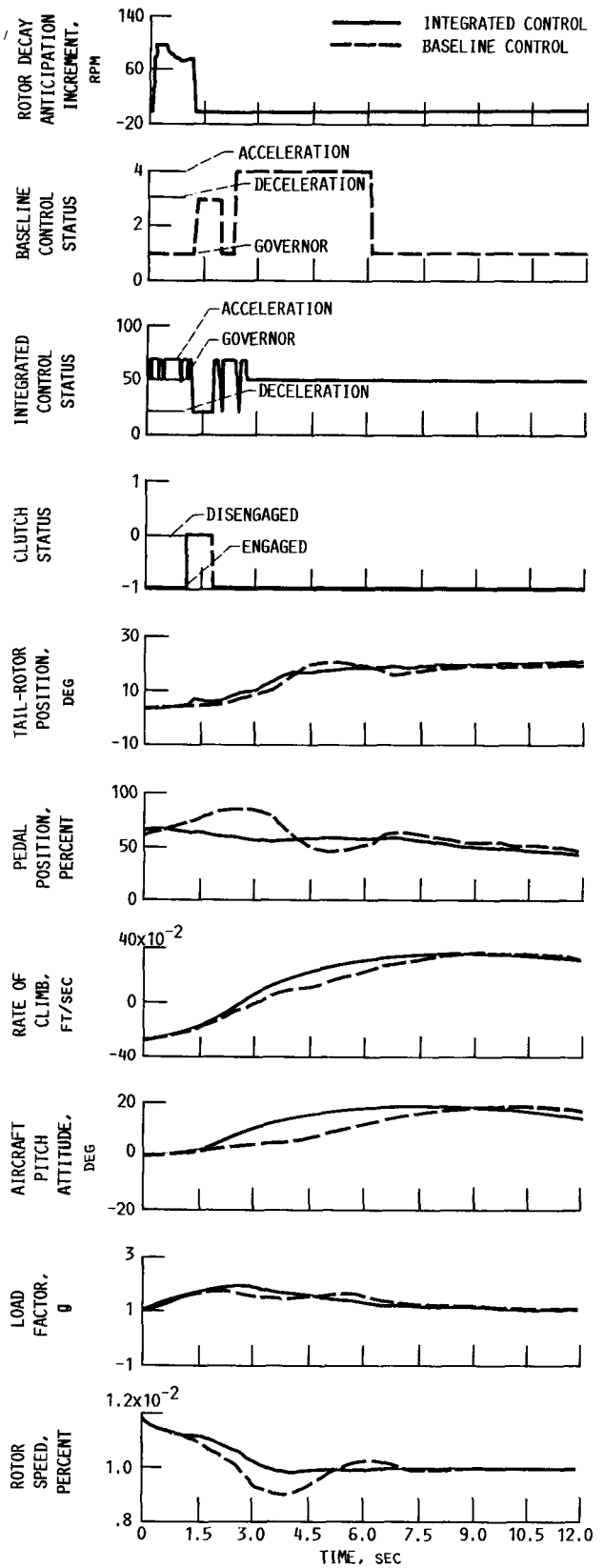

Figure 29.—Autorotational recovery from large speed split with slow collective pull.

Recovery with large split and fast pull: Figure 30 shows the same large split recovery using a much faster 0.5-sec pull. In this recovery, there is much less difference in behavior, with droop being reduced from 8 to 7 percent. The nose still goes higher with slightly more g pulled and the rudder activity clearly favors the integrated controller. Basically, the fast load demand spindle input slams both controller versions onto their acceleration schedule immediately. The rotor load increases quickly causing the shaft speed to decline so swiftly that the power turbines do not have time to overspeed, nor does the rotor decay compensation have time to speed up the gas generator. The result is that each system has to wait for the acceleration schedule to allow the engine to produce enough torque to overcome the droop. The LQR power turbine speed governor and droop recovery algorithms then make a much

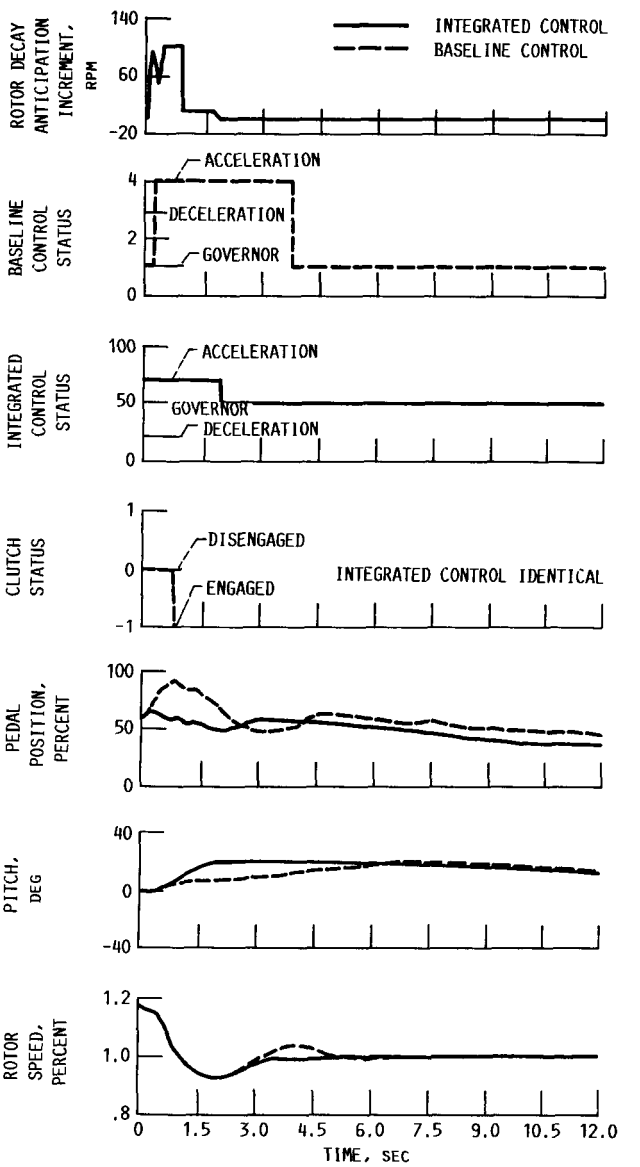

Figure 30.—Autorotational recovery from large speed split with fast collective pull.

better job of the subsequent recovery, allowing no overspeeding as opposed to 4.0 percent from the baseline control.

Recovery with small split and slow pull: Figure 31 shows a slow 3.0-sec pull recovery from the small split autorotation condition. The integrated control is rather worse than the baseline and allows a 4-percent droop as compared to 1 percent. This droop is largely due to deceleration schedule cycling of the integrated control with the gas generator reference speed of 102.5 percent. This occurs after clutch engagement at about 0.9 sec. This type of behavior seems to be a sensitivity problem that could be solved with additional design iterations.

Recovery with small split and fast pull: Figure 32 is the corresponding small split recovery using a fast 0.5-sec pull. The integrated control is again marginally worse than the baseline with 16 percent instead of 15 percent droop while the overspeed recovery is much better with 0.5-percent overspeed versus 4 percent. The pitch response is unrealistically severe. Pilot action would have been taken long before the nose rose to 30°. Basically, once again both controllers slam on to the acceleration schedule and stay there. The basic control stays there too long since it causes an overspeed at 4.5 sec while still on the acceleration schedule. The integrated control comes off its acceleration schedule at 2.2 sec and the subsequent recovery is smooth.

In summary, the integrated control is superior only during large split autorotational recoveries when moderate to slow

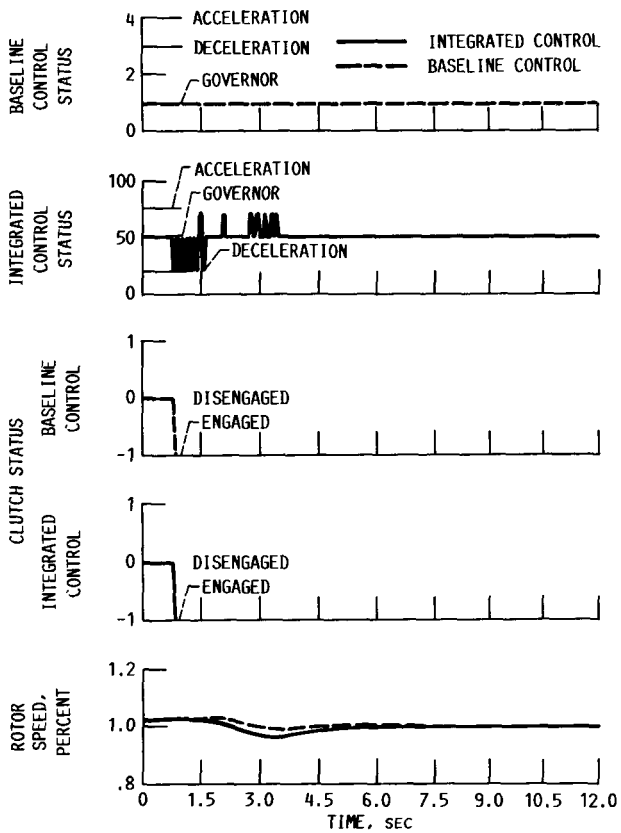

Figure 31.—Autorotational recovery from small speed split with slow collective pull.

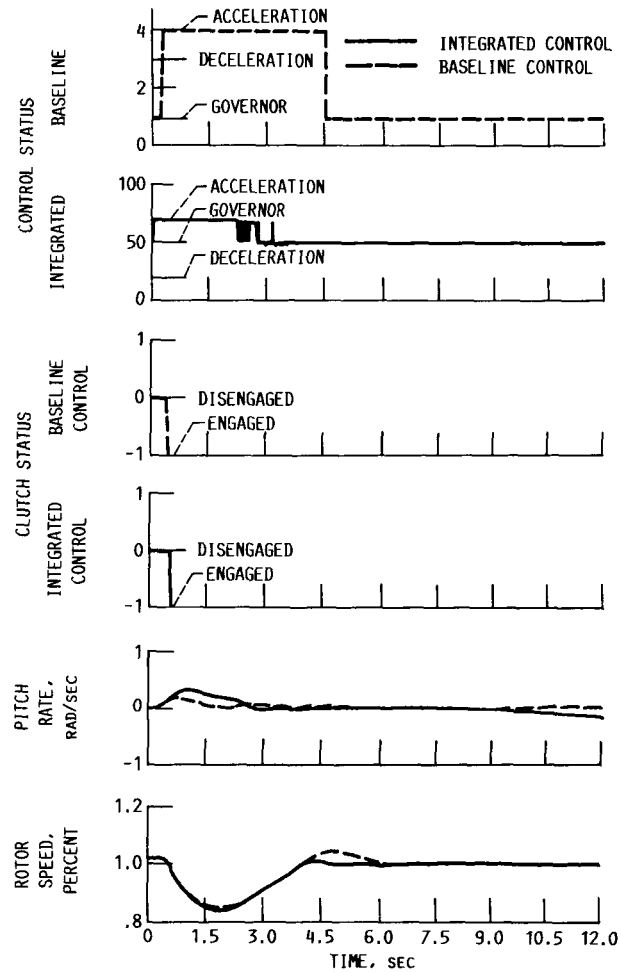

Figure 32.—Autorotational recovery from small speed split with fast collective pull.

collective pulls are used in the maneuver. Small split recoveries from fast to slow pulls do not show any significant advantage for either control version. However, rotor speed overshoot is controlled in a vastly superior manner by the integrated control. This fact is obviously due primarily to the LQR power turbine speed governor.

Bob-up and remask maneuver.—Figure 33 shows the simulated bob-up and remask maneuver flown using the maneuver controllers. A 5-percent overrun in collective pitch was not corrected. The height change was 55 ft and was achieved in 6 sec pulling a load factor in hover of about 1.9. The engine could respond quickly enough despite each control going onto its acceleration schedule almost immediately, and a 6-percent droop occurred. The baseline control stayed on its acceleration schedule for a full second longer than the integrated control with attendant overshoots twice as large. The LQR power turbine speed governor dealt with the situation more smoothly once the initial acceleration limited response was completed. This is further confirmed by the pedal movement plot where compensation was initially required because the rotor torque load came on before the engine

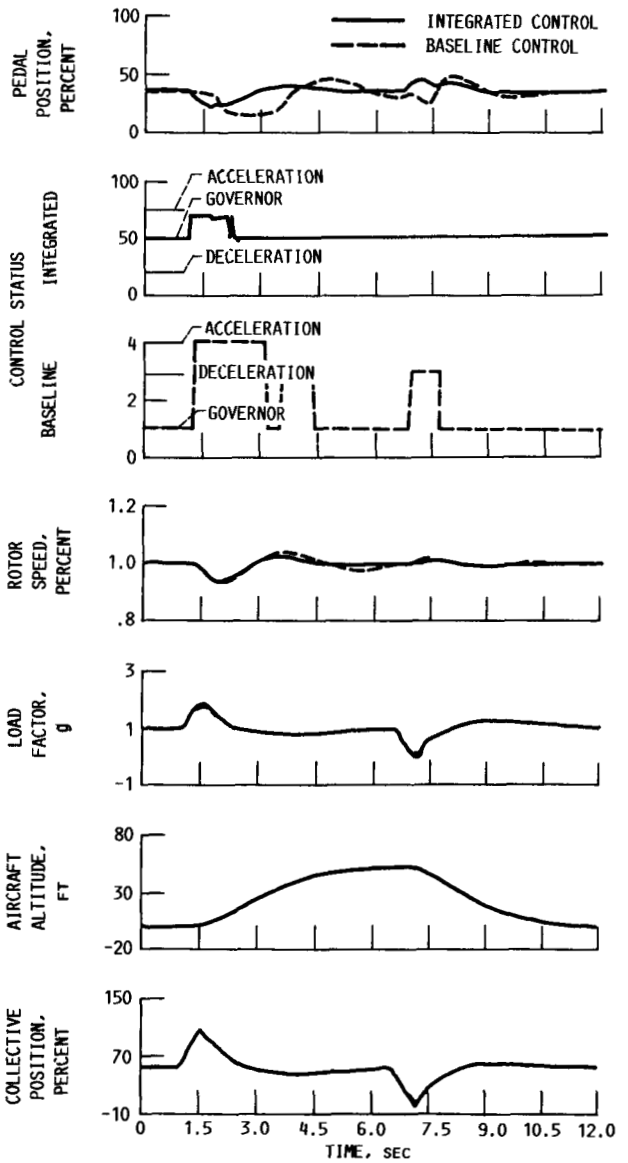

Figure 33.—Bob-up and remask maneuver.

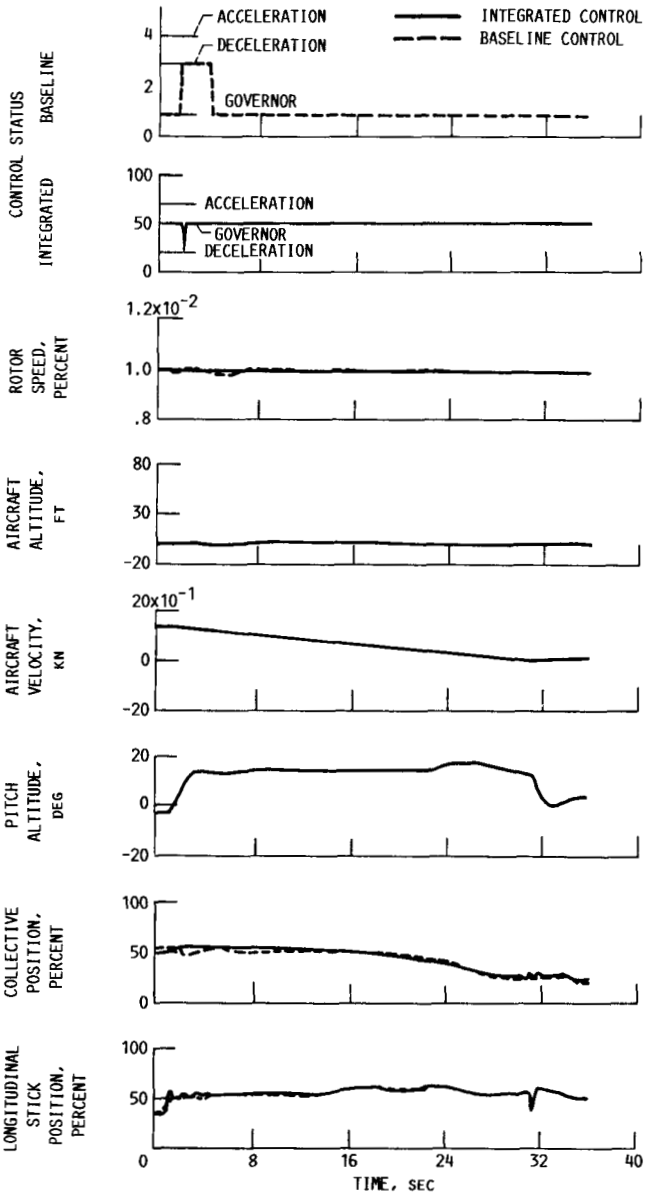

Figure 34.—Straight-line quickstop maneuver.

response. Later in the maneuver, the compensation came off smoothly until, briefly on the remask, the rotor load again changed faster than the engine response while on the deceleration schedule.

Straight-line quickstop maneuver.—Figure 34 is the simulated straight-line quickstop maneuver without altitude gain. The speed changes from 145 to 10 kn in 30 sec. The profile autopilot held the nose up 15° with the longitudinal stick until the speed dropped while maintaining a nominally zero rate of climb by dropping and then slowly increasing the collective pitch. The baseline governor went onto its acceleration schedule for about 2.5 sec and allowed about a 2-percent rotor droop. The LQR governor dealt with the loads without permitting any rotor droop with a momentary drop onto the deceleration schedule as collective pitch came down very fast at the 2-sec mark.

Sideward acceleration-deceleration maneuver.—Figure 35 is the simulated sideward acceleration-deceleration maneuver. The profile autopilot developed 40° of bank in one direction over 30 sec and reversed to 40° opposite bank in a further 2 sec and then rolled back to a recovery in hover. The bank angle was not left on for an appreciable time as only about 60 ft was traversed although roll rates of 60°/sec were developed. Neither controller had much difficulty with the loads developed although each allowed about 1.5-percent variation in rotor speed. The integrated control hit the maximum fuel flow limit and popped onto the acceleration schedule briefly as the stick was moved left at 3.7 sec to remove the right bank. The pedal yaw rate compensation was slightly more abrupt for the integrated control because the collective pitch compensation for constant altitude tended to

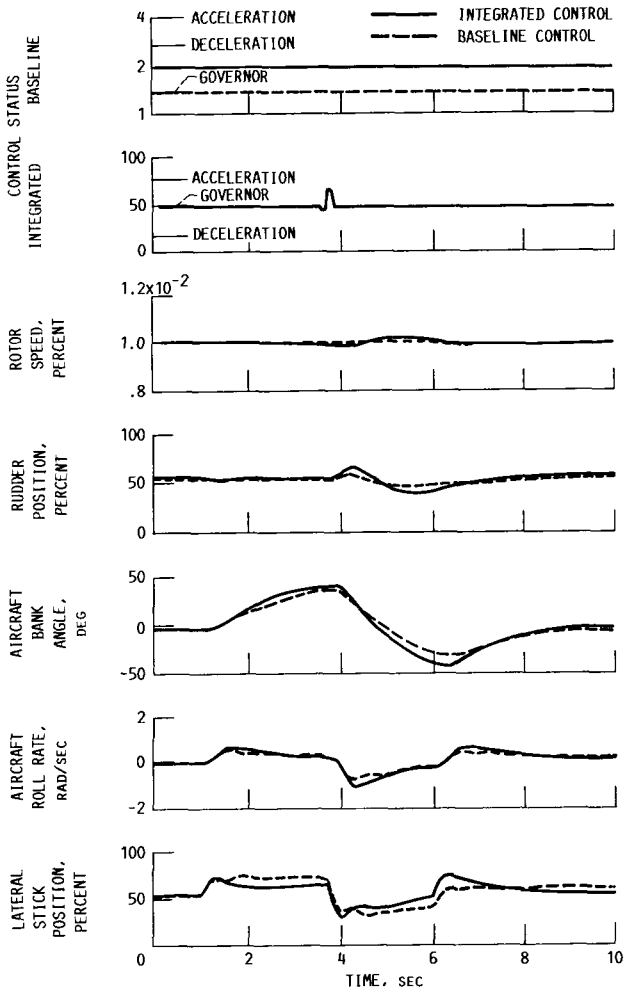

Figure 35.—Sideward acceleration-deceleration maneuver.

help the baseline linkage whereas the engine torque and phase lag tended to hinder the integrated control.

High-g turn.—Figure 36 shows the simulated high-g turn and deceleration maneuver flown by initiating and holding a 60° bank turn for a 180° heading change. Speed was bled off from 145 to 80 kn. The autopilot gains were rather higher than optimal, a condition which caused some unnecessry 1-Hz input excitation during initiation and recovery. There may also have been some undesirable coupling into the load factor enhancer, which was engaged at and after the 2-sec mark, which is seen to be holding rotor speed at about 7 percent above nominal during the turn load allowing the g pulled to approach 2.5. A 2-percent droop was seen for both controls during the final recovery.

Roll reversals.—Figures 37 and 38 show the simulated roll reversals for 50° right to 50° left and the opposite, respectively, as flown using the profile autopilot. The LQR governor exhibited good control during both of these maneuvers allowing just 1-percent droop during the most severe load change at 8 sec on figure 37 when the negative roll rate peaked at −45°/sec.

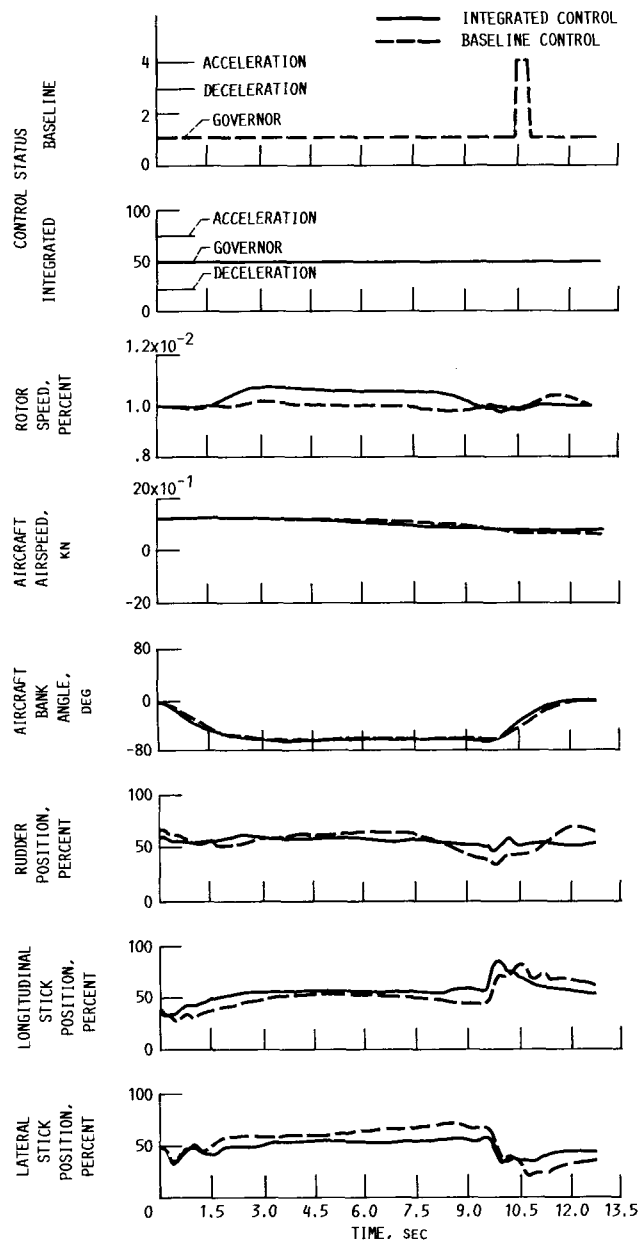

Figure 36.—High-g turn maneuver.

VMS Piloted Simulation Evaluation

A series of recommendations for VMS experiments to further evaluate the integrated control concept were made (Ruttledge, D.C.G.: Recommendations for VMS Experiments to Evaluate a Flight-Propulsion Control Integration Scheme. Sikorsky Aircraft Engineering Report, SER-760605, Apr. 1986). This work has not yet been accomplished. A full evaluation can only be performed with a real-time pilot-in-the-loop motion simulation.

The design of the integrated control system has been carried out entirely without pilot-in-the-loop simulation. Either simple control inputs or complex model-following maneuver controllers have been used to show the difference between the

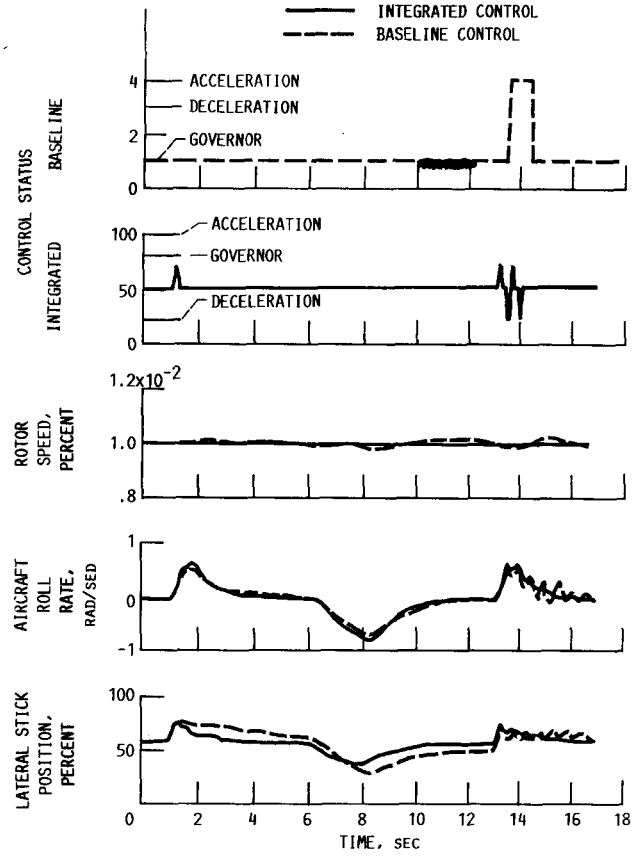

Figure 37.—Simulated roll-reversal maneuver; right-left-right.

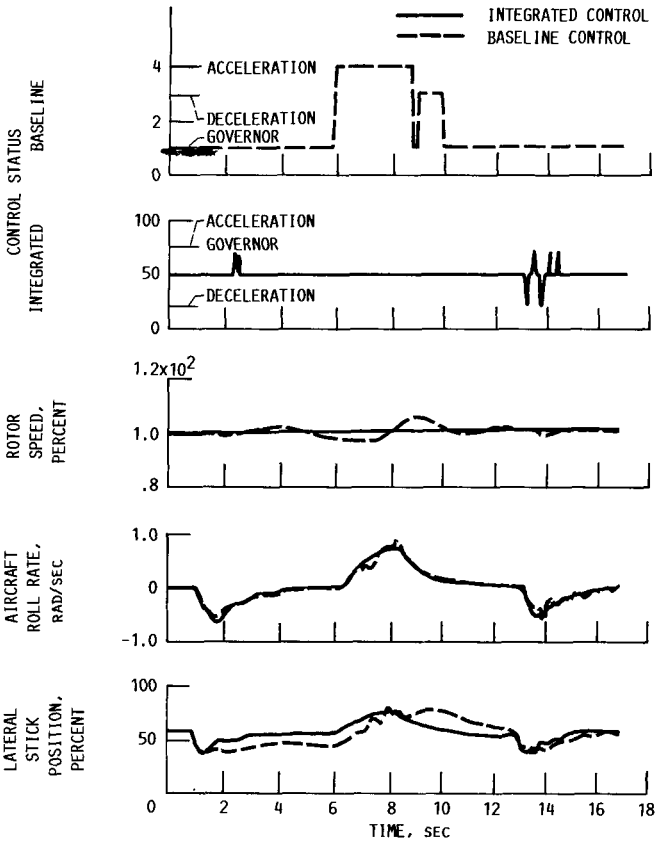

Figure 38.—Simulated roll-reversal maneuver; left-left.

basic control system and the integrated system. Such inputs can allow a theoretical quantitative assessment of the performance differences. However, the simple inputs are unrealistic in that they do not allow enough of a given maneuver to be flown without becoming excessively complex while the maneuver controllers, not having been designed as pilot equivalents, have a far too tight feedback loop set and cover up many shortcomings with their fast responses. A satisfactory multiaxis, full-flight-envelope paper pilot is not available, so a useful assessment of the integrated control system can only be made with a real pilot in the loop.

For example, in a typical high-g turn where the objective is to change the helicopter heading the least possible time, it is essential to slow down quickly while keeping other factors such as altitude and attitude within some bounds. In flight, it is common practice to employ large and varying amounts of slideslip induced by pedal inputs to achieve a more rapid speed reduction. The amount of pedal activity in this case is an important part of the assessment of the control system. Duplication of this maneuver using even sophisticated maneuver controllers is not possible yet it is not difficult for a pilot to fly it in a simulator. Similar arguments can be applied to other maneuvers which do not involve trivial motions. Maneuver controllers have a high bandwidth and are unrealistically fast.

A fixed-base simulator without motion would be adequate to investigate the basics of many of the aforementioned characteristics. However, as is always the case when such an experiment concerns control manipulations where primary cues to the pilot consist of accelerations, a moving-base simulator becomes essential to achieving the correct response of both aircraft and pilot. Here, in addition to the usual control response motion requirements, the presence of the rotor degree of freedom with associated droops and overspeeds and consequent out-of-trim motions and changes in control power make fixed-base simulation inadequate for assessing integrated flight-propulsion control concepts. With a moving-base simulator, motion cues, even of limited veracity, make the reasons for the difficulty of the task very apparent.

Recommended experiments.—The recommended experiments consist of flying a number of maneuvers used in the earlier design stages but with the addition of precision task requirements as far as practicable, and, of course, a pilot in the control loop. In each case, the baseline helicopter (the Black Hawk version at NASA Ames with the NASA T700 engine and control model) would be flown for comparison and, if deemed necessary, degraded to some extent to exemplify the differences in behavior between it and the integrated control version when a degraded airframe quality is predominating. With such degradation common to both helicopter control versions, it is hopeful that the integrated control would be more able to cope with the poorer characteristic. However, not too much can be done in this respect without moving away from

design parameters that would invalidate any comparison. For example, it would be reasonable to alter an aerodynamic surface at the tail but not to alter the rotor inertia.

Eight basic tasks are recommended for the evaluation:

(1) A quickstop maneuver that consists of stopping from various approach speeds within an NOE corridor followed by hover, a 10° bearing change, target acquisition, and weapon firing

(2) A low-level flight along a zig-zagging corridor at various constant speeds without adhering to the 45°-bank limitation of the Black Hawk

(3) A bob-up from hover to sight over a 150-ft obstacle, a left or right heading change through about 40°, aiming and firing a weapon at a target, and bobdown

(4) A sideflight NOE maneuver beginning from hover consisting of sighting a target through a screen, a fast translation across 500 ft or so keeping the heading near the target, recovery to hover, aiming and firing a weapon, and a fast return to cover

(5) A high-g turn maneuver provoked by a target appearing almost directly below the flight path while at cruise speed (which would require a turn in either direction through 270° as fast as possible), followed by target acquisition, weapon firing, and subsequent resumption of original flight direction (This maneuver should be flown with an altitude restriction and without a zoom turn.)

(6) Establishment of autorotational descents at various rotor speeds followed by a waved-off recovery

(7) Exercise of fuel minimization in high-speed cruise

(8) Observation of power available to hover during low-speed operation

All of these maneuvers should be flown in both still air and in a turbulent environment.

Expected results.—Task 1 is the simplest task and is designed to test the LQR governor and the tail rotor pitch link. Rotor autorotation could theoretically be reached, but practical pitch attitude limitations lead to milder torque load changes.

Task 2 also exercises the power turbine speed governor, the tail-rotor pitch link, and, at higher speeds, the rotor speed scheduling. The torque-spike anticipator discussed previously was not developed since it was quickly found that the LQR governor dealt adequately with the problem. The framework and inputs of these algorithms were left intact, however, and could be used if these tests indicate the necessity.

The course used should be sufficiently confining to ensure precision flying throughout. It should also be flown in reverse to evaluate the aircraft-system asymmetry due to the fixed rotor rotation. If the course proves too easy for the basic helicopter, a reasonable way of degrading the handling qualities for this task would be to reduce the vertical fin area. The resultant reduction would make the aircraft prone to Dutch roll and thus more difficult to fly precisely.

Task 3 exercises the power turbine speed governor. The requirement to reduce the rate of climb and make a heading change for a tracking task at the top of a bob-up is very demanding. The tail-rotor pitch link should reduce the pilot load slightly but will probably have to be learned to a degree since the timing will be different from that for the basic aircraft.

Task 4 again exercises the governor, but now, since collective-pitch movement is less than in the bob-up, the tail-rotor pitch linkage is relatively more important.

Task 5 adds the rotor speed scheduling to the governor and tail-rotor workload. The tail-rotor link is especially important since collective pitch may be required to be reduced to stop a climb while the rotor torque loading increases and holds with the prolonged steady g.

The recovery from the turn and coincident tracing task are difficult because the rotor might go into an autorotative state with the torque load changing very rapidly. This is a good test of the speed governor. The rotor speed scheduling will certainly need to be investigated thoroughly in this maneuver. The difference between a fixed-schedule and a proportional per-g controller can only be established on a practical basis by a pilot in the control loop.

Task 6 exercises the governor throughout the engine power range. This has traditionally been the most severe task for an engine governor since it can produce the most spectacular rotor speed droops and overshoots. In an autorotational landing, the droop and consequent reduction in control power occur in the flare just before touchdown, just at the wrong moment. This is a very demanding piloting task that cannot be eased by any changes to the engine governor design since the engine is offline. The waveoff or recovery from an autorotational descent required in this task brings the engine back online at some time during the torque load increase and consequent rotor speed decrease. A number of factors may have an effect during this time, leading to more or less subsequent rotor speed droop. High needle splits in the static autorotation may be conditionally better or worse in subsequent recovery than low splits and for different reasons. The basic Black Hawk seems to be more prone to rotor droop when recovering from small splits, but this may be due to pilot training. A precision task is not warranted during this maneuver, but good directional control will be a requirement and, if it is less than desirable, can be expected to be heavily criticized.

Task 7 sets up a number of cruise conditions and insures that the transient is negligible when switched on or off and that the routine correctly disconnects when stick inputs greater than 3 percent are held for more than 1 sec.

Task 8 monitors the power available to the hover indicator under different weight, altitude, and temperature conditions.

Concluding Remarks

The emergence of digital engine controls in such programs as the Army ATDE and the parallel development of digital flight controls in the Army ADOCS program make possible the future application of a fully integrated, digital flight and propulsion control system. Although the microelectronics

technology required for integrated control is now available, additional research is needed to understand the full implications of the technology. The NASA-Army research program described in this paper is a comprehensive attempt to develop an approach. The payoff will be a generation of rotorcraft with the maneuverability and agility required for military missions and the superior handling qualities and low pilot workload needed for all-weather civil missions.

The real-time individual-component digital simulation of a turboshaft engine fills a need in the pilot-in-the-loop investigations involving nonconstant rotor speeds and widely varying rotor loads especially in integrated control applications. Performance-related questions can also be addressed in real-time. The model reproduces dynamics associated with gas generator spoolup or spooldown caused by large changes of power. Engine degradation is also easily modeled by modifying compressor or turbine flow and energy functions. The engine control system is separate and may be modified or replaced depending on user requirements. This capability allows effective pilot evaluations of new control implementations or of special modes of fuel control system operation.

The integrated flight-propulsion control scheme evaluated using MGH in this study was found to be superior to the basic control in most areas. This was in spite of the fact that the baseline control is already a harmonious match of engine and airframe, which exhibits few of the problems of other aircraft on a diminished scale as seen in the AACT data.

While MGH provides a useful tool for the preliminary investigations of control studies such as this, the essence of the evaluation has to be a motion simulation because the critical factor is the extent to which rotor speed droop affects control power and how a pilot copes with the subsequent control problem. To this end, a simulation experiment on a motion simulator in real-time is necessary.

An eclectic approach of selecting versions of elements already existing results in many design compromises that should not have to be made. It is strongly recommended that airframe, engine, and controls teams establish a small integrated design team at the start of a program to deal with all aspects of the required integration concepts using modern, integrated control design methodologies that have emerged in recent times. Variable rotor speed control, which will require integrated control to be implemented effectively, should also be the object of further study.

Lewis Research Center
National Aeronautics and Space Administration
Cleveland, Ohio, January 28, 1988

References

1. Richardson, D.A.; and Alwang, J.R.: Engine/Airframe/Drive Train Dynamic Interface Documentation. USARTL-TR-78-11, 1978. (Avail. NTIS, AD-A055766).
2. Needham, J.F.; and Banerjee, D.: Engine/Airframe/Drive Train Dynamic Interface Documentation. USARTL-TR-78-12, 1978. (Avail. NTIS, AD-A056956).
3. Twomey, W.J.; and Ham, E.H.: Review of Engine/Airframe/Drive Train Dynamic Interface Development Problems. USARTL TR-78-13, 1978. (Avail. NTIS, AD-A057932).
4. Bowes, M.A.: Engine/Airframe/Drive Train Dynamic Interface Documentation. USARTL TR-78-14, 1978. (Avail. NTIS, AD-A058197).
5. Hanson, H.W., et al.: Engine/Airframe Drive Train Dynamic Interface Documentation. USARTL-TR-78-15, 1978. (Avail. NTIS, AD-A063237).
6. Landis, K.H.; and Glusman, S.I.: Development of ADOCS Controllers and Control Laws. (D210-12323-VOL-1,-2,-3, Boeing Vertol Co.; NASA Contract NAS2-10880), NASA CR-177339-VOL-1,-2,-3, 1984.
7. Corliss, L.D.: A Helicopter Handling-Qualities Study of the Effects of Engine Response Characteristics, Height-Control Dynamics, and Excess Power On Nap-Of-The-Earth Operations. Helicopter Handling Qualities, NASA CP-2219, 1982, pp. 47-57.
8. Corliss, L.D.: The Effects of Engine and Height-Control Characteristics On Helicopter Handling Qualities. AHS J., vol. 28, no. 3, July 1983, pp. 56-62.
9. Corliss, L.D.; Blanken, C.L.; and Nelson, K.: Effects of Rotor Inertia and RPM Control on Helicopter Handling Qualities. AIAA Paper 83-2070, Aug. 1983.
10. Sellers, J.F.; Baez, A.N.; and Bobula, G.A.: Army/NASA Small Turboshaft Engine Digital Controls Research Program. NASA TM-82979, 1981.
11. De Los Reyes, G.; and Gouchoe, D.R.: The Design of a Turboshaft Speed Governor Using Modern Control Techniques. NASA CR-175046, 1986.
12. Morrison, T.; Zagranski, R.D.; and White, A.H.: Adaptive Fuel Control Feasibility Investigation. USAAVRADCOM-TR-83-D-1, July 1983. (Avail. NTIS, AD-B076297L).
13. Yates, T.W.: Adaptive Fuel Control Feasibility Investigation. USAAVRADCOM-TR-82-D-39, July 1983. (Avail. NTIS, AD-B075819L).
14. Steininger, S.A.; Zagranski, R.D.; and Morrison, T.: Adaptive Electronic Fuel Control for Helicopters. USAAVSCOM-TR-86-D-14, Dec. 1986. (Avail. NTIS, AD-B110026L).
15. Ruttledge, D.C.G.: A Rotorcraft Flight/Propulsion Control Integration Study. (SER-760606, Sikorsky Aircraft; NASA Contract NAS3-24343) NASA CR-179574, November 1986.
16. Howlett, J.J.: UH-60A Black Hawk Engineering Simulation Program: Volume I--Mathematical Model. (SER-70452, Sikorsky Aircraft; NASA Contract NAS2-10626), NASA CR-166309, 1981.
17. Hull, R.: Development of a Rotorcraft Propulsion Dynamics Interface Analysis: Volume 1. NASA CR-166380, 1982.
18. Kaplita, T.T.: UH-60 Black Hawk Engineering Simulation Model Validation and Proposed Modifications. (SER-70982, Sikorsky Aircraft; NASA Contract NAS2-11570). NASA CR-177360, 1985.
19. Hart, C.E.; and Wenzel, L.M.: Real-Time Hybrid Computer Simulation of a Small Turboshaft Engine and Control System. NASA TM-83579, 1984.
20. Seldner, K.; Mihaloew, J.R.; and Blaha, R.J.: Generalized Simulation Technique for Turbojet Engine System Analysis. NASA TN D-6610, 1972.
21. Mihaloew, J.R.; and Hart, C.E.: Real Time Digital Propulsion System Simulation for Manned Flight Simulators. AIAA Paper 78-927, July 1978. (NASA TM-78958).
22. Mihaloew, J.R.: A Nonlinear Propulsion System Simulation Technique for Piloted Simulators. NASA TM-82600, 1981.
23. French, M.W.: Development of a Compact Real-Time Turbofan Engine Dynamic Simulation. SAE Paper 821401, Oct. 1982.
24. Alwang, J.R.; and Skarvan, C.A.: Engine Control Stabilizing Compensation-Testing and Optimization. AHS J., vol. 22, no. 3, July 1977, pp. 13-18.
25. Howlett, J.J.; Morrison, T.; and Zagranski, R.D.: Adaptive Fuel Control for Helicopter Applications. AHS J., vol. 29, no. 4, Oct. 1984, pp. 43-54.

NASA
National Aeronautics and Space Administration

Report Documentation Page

1. Report No.	2. Government Accession No.	3. Recipient's Catalog No.
NASA TP-2815		

4. Title and Subtitle	5. Report Date
Rotorcraft Flight-Propulsion Control Integration: An Eclectic Design Concept	April 1988
	6. Performing Organization Code

7. Author(s)	8. Performing Organization Report No.
James R. Mihaloew, Mark G. Ballin, and D.C.G. Ruttledge	E-3812
	10. Work Unit No. 505-63-51

9. Performing Organization Name and Address	11. Contract or Grant No.
National Aeronautics and Space Administration Lewis Research Center Cleveland, Ohio 44135-3191	
	13. Type of Report and Period Covered Technical Paper

12. Sponsoring Agency Name and Address	14. Sponsoring Agency Code
National Aeronautics and Space Administration Washington, D.C. 20546-0001	

15. Supplementary Notes

James R. Mihaloew, NASA Lewis Research Center; Mark G. Ballin, NASA Ames Research Center, Moffett Field, California 94035; D.C.G. Ruttledge, Sikorsky Aircraft Division, United Technologies, Stratford, Connecticut 06601.

16. Abstract

The NASA Ames and Lewis Research Centers, in conjunction with the Army Research and Technology Laboratories, have initiated and partially completed a joint research program focused on improving the performance, maneuverability, and operating characteristics of rotorcraft by integrating the flight and propulsion controls. The background of the program, its supporting programs, its goals and objectives, and an approach to accomplish them are discussed in this report. Results of the modern control governor design of the General Electric T700 engine and the Rotorcraft Integrated Flight-Propulsion Control Study, which were key elements of the program, are also presented.

17. Key Words (Suggested by Author(s))	18. Distribution Statement
Integrated controls Rotorcraft	Unclassified – Unlimited Subject Category 08

19. Security Classif. (of this report)	20. Security Classif. (of this page)	21. No of pages	22. Price*
Unclassified	Unclassified	33	A03

NASA FORM 1626 OCT 86

*For sale by the National Technical Information Service, Springfield, Virginia 22161

NASA-Langley, 1988